Biodegradable magnetic actuator for mechanical stretching of cells in organs-on-chip

Zhengwei Liao

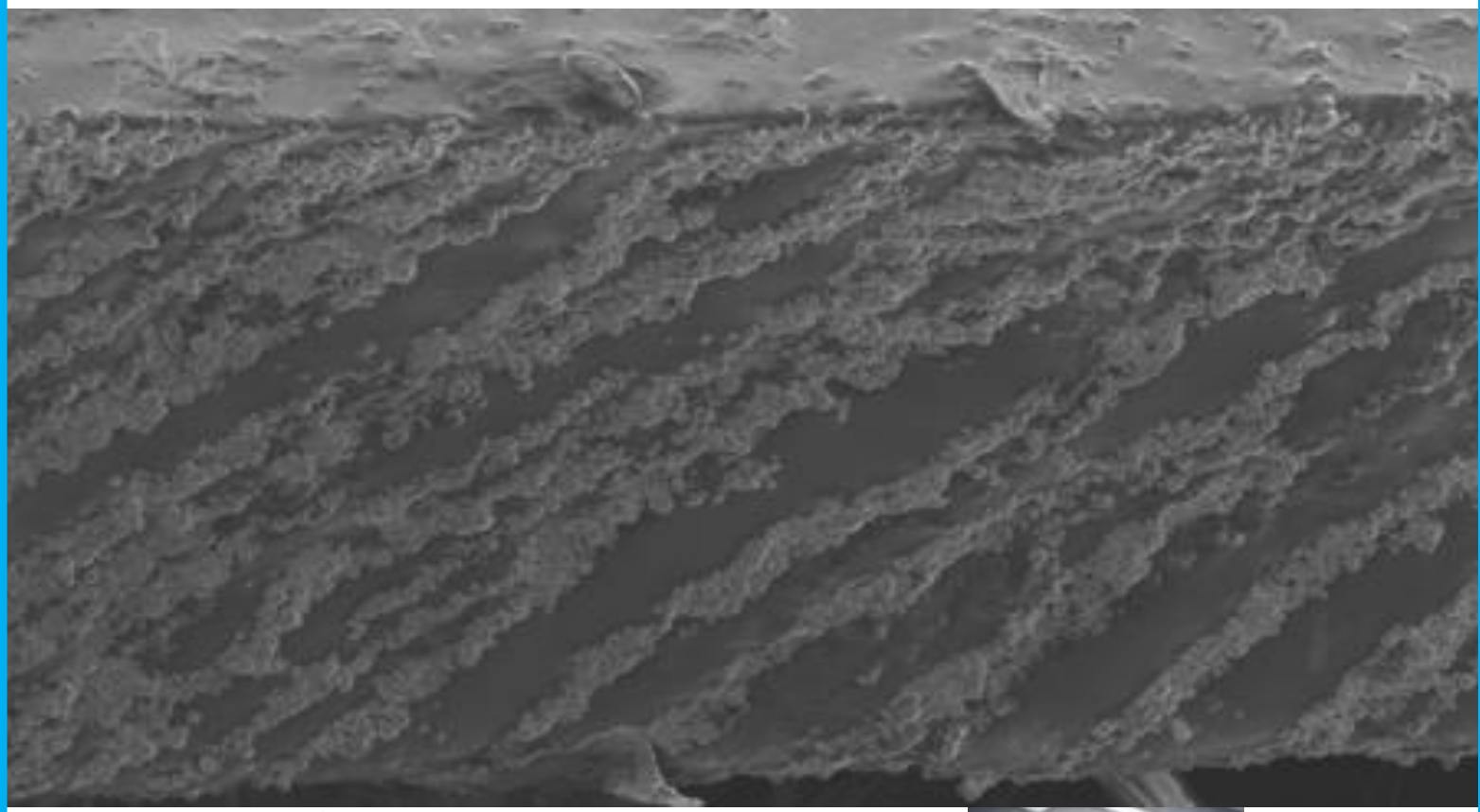

TU Delft

Materials Science and Engineering

ECTM

Challenge the future

Biodegradable magnetic actuator for mechanical stretching of cells in organs-on-chip

By

Zhengwei Liao

to obtain the degree of Master of Science in Material Science and Engineering
at the Delft University of Technology,
to be defended publicly on 26/8/2022 at 10 AM.

Student number: 5229758
Project duration: Dec 1, 2021 – Aug 26, 2022
Thesis committee: Dr. Clementine Boutry, TU Delft, supervisor
Dr. Jilt Sietsma, TU Delft, co-supervisor
Dr. Lina Sarro, TU Delft, committee member

Acknowledgements

Before taking you into my research result of my 9-month thesis, I would like to show my gratitude to several people.

Firstly, I would like to express my thanks to prof. Clementine Boutry, my supervisor, for proving this interesting research direction, giving patient instructions and enough research freedom. Thanks for offering me the opportunity to be the first one to join your group. I firmly believe that you will succeed as a professor in near future. I would sincerely thank my co-supervisor, prof. Jilt Sietsma. I do benefit a lot from discussing with you about thesis process, specific experiments, and technical question. I know you are very busy as a big leader in MSE but you can always find time to meet with me. I wish you good health and enjoy your retired life after 2022.

Secondly, supports from ECTM group and EKL do help me a lot. Thank prof. Massimo for giving me some guidance during our daily talks and in group meeting. Thank Bjorn for giving me patient instruction about the 3D printing machine. I also want to show thank my colleagues, Oualid, Francesco and Matteo. You helped me not only on the thesis but also about the daily life and some emotion problems. I do learn a lot from you. Especially thank Oualid, the discussions with you give me many inspirations. I also want thank all the technicians in EKL and ECTM including Hitham, Filip and so on.

Finally, I want to express my big thank to my parents, Cuixia and Quanbo, who give me financial and emotional support so that I can study in TUDelft. Thank you Yunrui. As a girlfriend, she gives me a lot of support and help.

Abstract

Organ-on-chip (OoC) is invented around 10 years ago which is used to do pre-clinical drug test without live animals. Physiological microenvironment of different cells can be mimicked in OoC. In order to better form of tissue in OoC, mechanical stimulation can offer through different ways including pneumatic, thermal, and electric stimulations. As another way to offer mechanical deformation, magnetic stimulation has high reacting speed and wireless operation.

This thesis aims to fabricate a composite substrate of OoC which can offer magnetic stimulation in magnetic field. Carbonyl iron particle (CIP) and poly (octamethylene maleate (anhydride) citrate) (POMaC) are used as magnetic particle and elastomer substrate for OoC scaffold. POMaC is synthesized successfully and the pure POMaC substrate and POMaC/CIP composite substrate are fabricated. For POMaC/CIP sample, CIP chain distribution is realized inside the substrate through a tilted magnet. Besides, the mechanical property, magnetic property, substrate structure and degradation property are characterized. Finally, the mechanical reaction of POMaC/CIP substrate to magnetic field is investigated. POMaC/CIP substrate shows close mechanical property to muscle cell and strong magnetic response. Its reaction to magnetic field also accords with its chain distribution.

Content

1
Introduction

Pre-clinical drug test is still mainly based on animals. It is expensive and ethically controversial although it is the closest model to human. However, comparing to human body it mimics physiopathology of human beings less precisely [1]. Ten years ago, organ-on-chip (OoC) was named by Prof. Donald and his coworkers for the first time [2]. The function of OoC is to mimic complex physiological microenvironment of different cells and culture cells to become mature tissue. If human tissue can be cultured in OoC, it can be used directly for pre-clinical drug test. An example of OoC is shown in figure 1a. The scaffold which the cells grow on is an important part in OoC. For successfully mimicking in-vivo environment in the scaffold, many factors like mechanical properties, structure, and biocompatibility need to be taken in consideration [3]. In this particular example [4], the cells are seeded in a suspended scaffold, inserted into a polydimethylsiloxane (PDMS) well. Growth situation of cells can be observed through transparent polycarbonate body. Polycarbonate base can be used to stabilize the whole system, while the cap is used to seal it. An example of seeding cells is shown in figure 1b where endothelial and parenchymal cells are cultured in scaffold. They diffuse and gradually seed everywhere the scaffold. A more detailed schematic of cells on scaffold is shown in figure 1c. Yellow part is scaffold composed of channels, holes, and pores. Parenchymal cells grow around scaffold surface and porous areas. After culturing for certain time, cells grow into tissue and become ready for drug test.

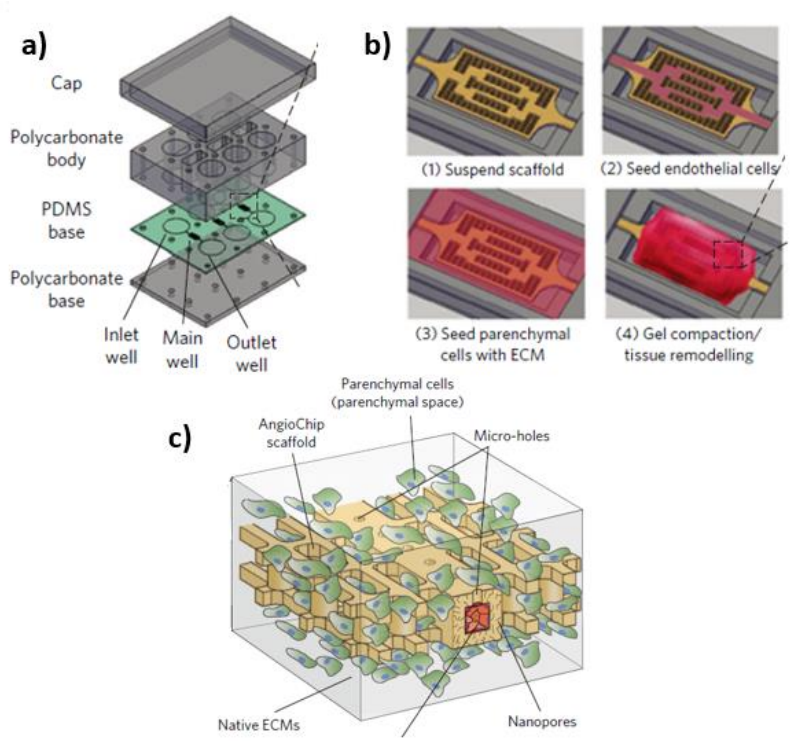

Figure 1. **Detailed Structure of organ-on-chip.** a) Schematic of OoC structure. b) Image of cultured vascularized tissue. c) Parenchymal cells growing around scaffold [4].

For better tissue formation in OoC, mechanical stimulation is needed for better mimicking microenvironment of cell growth [5], especially for muscle cells which experience mechanical strain continuously in human body. Therefore, required strain for cell growth in vitro and the way to offer this strain are two important aspects in OoC. The first aspect is about biologically requirement while the second aspect is related to actuator. There are many ways to offer controlled mechanical deformation in flexible device including pneumatic, thermal, electrical, and optical stimulation. Magnetic field is another type of stimulation to generate deformation. High reacting speed and wireless operation are its advantages. It is also biological friendly because magnetic field does not harm human body if the intensity is not too high [6].

In the thesis, biodegradable magnetic actuator substrate is fabricated and characterized. It is composed of carbonyl iron particle (CIP) and poly (octamethylene maleate (anhydride) citrate) (POMaC) where CIP has suitable magnetic property and POMaC is a good elastomer. Firstly, POMaC is synthesize and CIP is characterized. Both pure POMaC samples and POMaC/CIP samples are fabricated. Structure, mechanical

property, magnetic property, and biodegradable features of thin film samples are measured. Finally, perpendicular magnetic field is applied to POMaC/CIP sample in order to test the deformation situation. A schematic of the fabricated POMaC/CIP biodegradable magnetic actuator substrate is shown in figure 2.

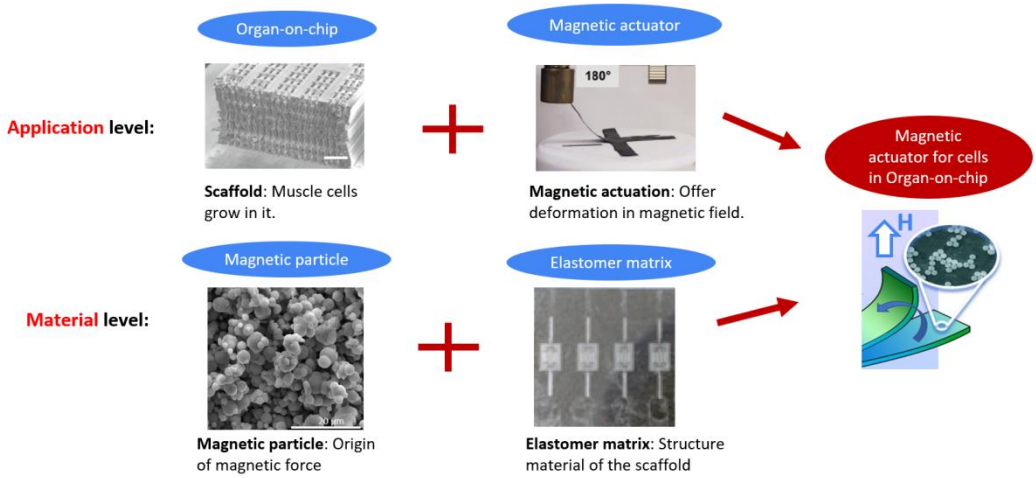

Figure 2. Structure of fabricated POMaC/CIP sample from both application and material level. For top left figure, the scale bar is 1mm while the scale bar of bottom left one is 20 μm [4].

2

Background

2.1 Needed strain for muscle cells culturing

For drug test in OoC, tissues are cultured in vitro. Additional mechanical stimulation can better mimicking biology environment of cell in vitro, so that cell growth can get improved comparing with the static cells in vitro. In this section, information about the mechanical strain used for skeletal and myocardium cells growth is summarized. Through the information shown in the tables, proper mechanical strain used for certain cells is discussed. For all the strain condition below, the minimum value in strain range is 0%.

2.1.1 Skeletal muscle cells

Considering the responsiveness to mechanical stimulation, skeletal cell is very critical in our body [7]. Skeletal tissue generates contractile force spontaneously in human body which is transmitted through muscle network. Therefore, for culturing mature skeletal tissue in OoC, cyclic mechanical strain is important. Table 1 shows the stretching parameters selections for the optimal growth of skeletal muscle cells cultured in vivo [7]. All the growth situations of stimulated cells in table 1 are comparing with the growth of static cells. From the result of Liu et al. and Clarke et al. [8], [9], too large strain may induce cell damage. 20% may be the maximum value of applied strain. Kurokawa et al.[10] tested the influence of strain rate on cell proliferation and differentiation. Strain rate does not show obvious influence on the number of cells which is one indicator of proliferation. It was also concluded that proliferation of stimulated cells is prompted comparing with controlled cells. Additionally, differentiation is observed through detecting the expression of myosin heavy chain (MyHC)-perinatal which is a type of mRNA used to determine the differentiation speed of myoblast. Measurement result shows that strain rate does not influence

differentiation. Kumar et al. [11] reported that 17% strain restrained differentiation into myotubes which means that myogenesis is inhibited. Experiment results shows that it is caused by the activation of nuclear factor and focal adhesion kinase.

Therefore, as for proper mechanical stimulation needed for better skeletal cell growth, strain value and strain rate should be around 15% and 0.5 Hz respectively.

Table 1. Summary about some researches regarding the stretched muscle precursor cells.

Cell type	Stretching parameters	Key Finding	Reference
Murine myoblast (C2C12)	15%, 0.5 Hz	Increased cell number (at least 20%) comparing with controlled cells which means higher proliferation.	Iwanuma et al [12]. (2008)
Murine myoblast (C2C12)	17%, 1 Hz	Stretch increased proliferation (increased number of cells around 40%) and inhibited differentiation	Kumar et al [11]. (2004)
Murine myoblast (C2C12)	15%, 0.1, 0.5, and 0.9 Hz	Stretch stimulation increase the number of myoblast (at least 20%) and myoblast nuclei (at least 50%). Different strain rate does not show different influence on proliferation and differentiation.	Kurokawa et al [10]. (2007)
Rat myoblasts (L6)	20%, 0.5 Hz	Stretch caused apoptosis during differentiation	Liu et al [9]. (2009)
Human MDCs	10%–20% cyclical strain	Acute stretching caused membrane wounding.	Clarke and Feeback [8]. (2008)

2.1.2 Myocardium cells

Heart is one of the most investigated organs. Cardiomyocytes in vivo are subjected to contraction because of continuous heartbeat. This type of macroscopic contraction is

transmitted to every cardiomyocyte through uniaxial deformation [13]. It is already reported that mechanical stimulation improves self-assembly, maturation, and functionality of cardiomyocyte tissues [14]. Therefore, in order to culture robust and mature cardiomyocyte tissue proper mechanical stimulation is important. Table 2 shows the stretching parameters selections for the optimal growth of myocardium cells cultured in vivo. Zhang et al. [4] did uniaxial tensile experiment on rat ventricular myocardium. Result is shown in figure 3a. Strain and stress present almost linear relationship before strain reaches 15%. Deviation from linear part at high strain may be caused by plastic deformation or some tensile induced damage in cells which does not happen in vivo. Because Rappapor et al. [15] also reported that physiological strain (reversible) experienced by normal heart does not exceed 15% which is consistent with the result in figure 3a. Zhao et al. [16] applied cyclic strain (10%, 1Hz) on rat cardiomyocytes. Functionality of formed tissue is tested by measuring the expressions of cardiac-specific proteins. Result shows that 10% strain stimulation prompts functionality effectively. Chen et al. [17] researched the effect of cyclic strain on the expression profile for gene. Result shows that the number of some genes is up-regulated while some are down-regulated. Through certain analysis, it is found that cardiac cell metabolism is accelerated when strain is applied. Marsano et al. [18] stimulated cardiac cells with certain strain (10%, 1Hz). In figure 3b, cells in 3 different areas can all spontaneously contract. However, only the stimulated one shows synchronous contraction. Besides, two tracings in figure 3c also show that the stimulated cells contract with higher rate which is 2 times as much as the controlled cells. In figure 3d, stimulated one shows more complex structure where intercalated discs and gap junctions can be found.

Overall, mechanical stimulation can improve functionalities and maturity of cardiac cell. However, too much strain should be avoided. Summarized from above analysis, mechanical stimulation with about 15% strain amplitude and 1 Hz may be a proper value for better in-vitro cardiomyocyte growth.

Table 2. Summary about some researches regarding the stretched myocardium cells

Cell type	Stretching parameters	Key Finding	Reference
Adult rat ventricular myocardium	0-20%, static strain	Cells are damaged when strain is higher than about 15%	Zhang et, al [4]. (2016)
Isolated neonatal rat cardiac cells	10%, 1Hz	Stimulated cells show higher viability, more complex organization, and better contractile property	Marsano et, al [18]. (2016)
Neonatal isolated rat cardiomyocytes	10%, 1Hz	Mechanical stimulation promotes the functionalities (including organized tissue and gap junctions) of generated cardiac tissue.	Zhao et [16], al. (2019)
Human ventricular cardiomyocyte cells	15%, 0.5Hz	Cyclic stretching effectively changes the expression profile for gene.	Chen et [17], al. (2020)

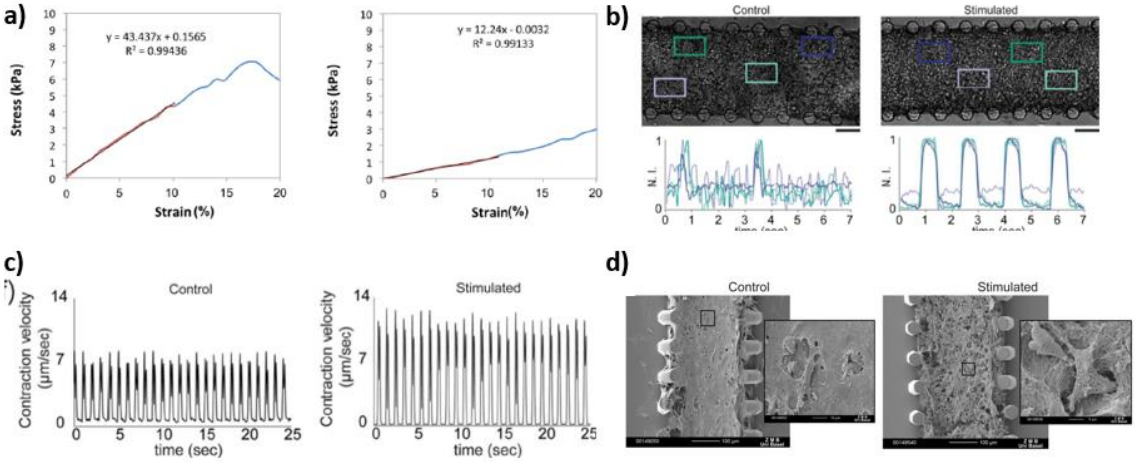

Figure 3. **Effect of stretching on myocardium cell.** a) Uniaxial tensile stress-strain plots of adult rat ventricular myocardium. Left one is for cells along long-edge direction while right curve is short-edge direction. Red line corresponding to the linear fitting result from 0-10%. Linear regression equation and R-value are also shown in the figure [4]. b) Contractile activity of multiple randomly selected regions in the rat cardiomyocytes constructs with (right) and without (left) mechanical stimulation (cyclic uniaxial strain: 10%, 1Hz) [18]. The scale bar is 100 μm. c) Contraction velocity of cardiomyocytes micro-tissues without mechanical stimulation (left) and after cyclic uniaxial strain (right) [18]. d) (Scanning electron microscope) SEM image of mechanically stimulated (right) and control (left) myocardium cells cultured for 6 days on extracellular matrix [18].

2.2 Magnetic actuation of elastomer filled with magnetic particles

In this section, composite material, magnet setup, actuation mechanism, fabricating methods and deformation methods for anisotropic magneto-sensitive elastomer film (MSEF) composite filled with magnetic particles will be discussed. MSEF can present many kinds of actuations under external magnetic field. Besides, it is present in many magnetic actuators [19]. Its magnetic anisotropy is the origin of deformability. Elastomer filled with aligned magnetic particles is an important category of MSEF. Many actuations are realized through different magnetic profiles [20]–[23]. Particles in the matrix are programmable which means that different particle distributions can be realized through applying different magnetic fields. Therefore, many different actuations can be realized.

2.2.1 Particle and matrix material for magnetic actuation

As mentioned above, the composite magnetic film that composes of matrix and particles is our research object in this report. Properties of both two materials will be illustrated in the following two parts respectively. In order to fulfill the requirement of OoC application, matrix material needs to be biodegradable and elastomer. For the particle inside, proper magnetic property is required.

2.2.1.a Magnetic particle materials

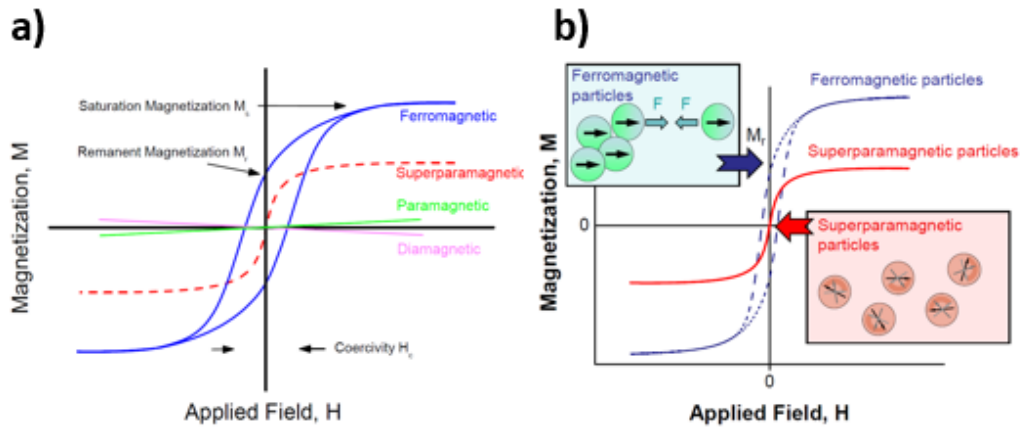

Figure 4. **Different magnetisms and magnetic properties of material.** a) M-H curves of ferromagnetism, paramagnetism, superparamagnetism and demagnetism [24]. b) Schematic of magnetic property and agglomeration behavior of ferromagnetic and superparamagnetic particles

[24].

Many types of magnetic particles are used in polymer soft magnetic actuator, including superparamagnetic, paramagnetic, and ferromagnetic particles [25]. The difference between different magnetisms are shown in figure 4a [24]. For ferromagnetism, high saturation magnetization is its advantage comparing with other magnetic properties. Large remanent and coercivity are another two features of ferromagnetic materials as shown in the curve. However, high remanent makes particles attract each other and generates agglomeration which is not favorable in composite film. For paramagnetism, it is the opposite of ferromagnetism. Paramagnetic material does not show magnetization when no magnetic field is applied. Besides, its saturation magnetization is much lower than ferromagnetic material.

In order to avoid particle agglomeration and keep enough magnetization simultaneously, superparamagnetic particle is a proper option for MSEF composite filled with magnetic particles. Superparamagnetic particle shows ignorable remanent and coercivity. Its magnetization is lower than ferromagnetic but it is enough for some magnetic actuations [21], [22]. Superparamagnetism is small particle effect of ferromagnetic material. Below 50 nm is the typical size of superparamagnetic particles where only one magnetic domain exist [26]. Magnetic moment tends to be aligned with the easy axis of particle when no magnetic field is applied. The needed energy to hold magnetic particle away from easy axis is named anisotropy energy which is proportional to the volume of particle. When particle size is small enough, thermal motion energy can overcome the anisotropy energy. Therefore, magnetic moment can point in any direction because of the random flipping caused by thermal motion which make particles show paramagnetism instead of ferromagnetism [27]. This type of paramagnetism is named superparamagnetism as it shows higher magnetization than normal paramagnetic material. Different from ferromagnetic particles, remanent magnetization of superparamagnetic particles is ignorable which contributes to stable and uniform particle dispersion in matrix [24]. Therefore, superparamagnetic particle is favorable for composite magnetic actuator. Figure 4b shows particles attraction of ferromagnetic particle and random flipping of superparamagnetic particles.

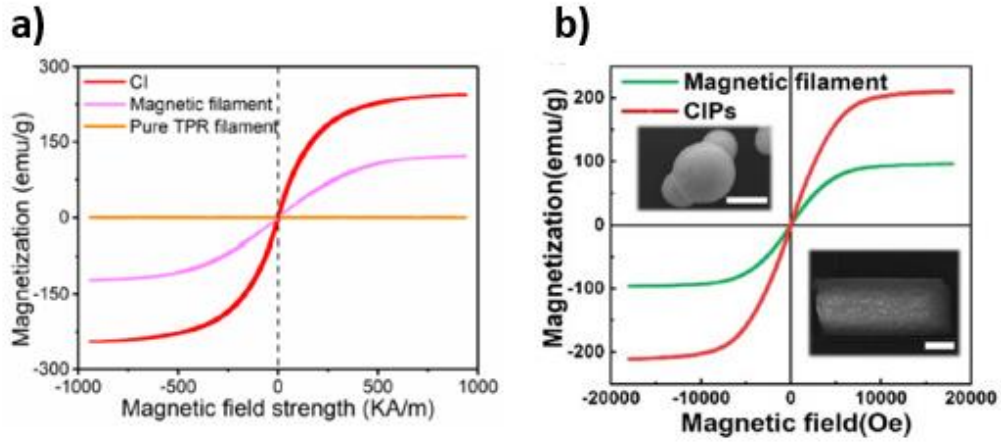

Figure 5. **Magnetization curves of carbonyl iron particles.** a) M-H curves of carbonyl iron particles (CIPs), magnetic filament and pure TPR filament [28]. b) M-H curves and SEM images of CIPs and magnetic filament. Scale bars are 2 μm and 0.5 mm [20].

Prof Metin and his coworkers reported a magnetic hydrogel gripper with superparamagnetic iron oxide nanoparticles (10 nm diameter) which can offer enough magnetization for grasping 7.5 mg object [22]. For further increasing magnetization of superparamagnetic particles by increasing its size, J. Ge et al. introduced a method to synthesize magnetite colloidal nanocrystal clusters (CNCs) with maximum 120 nm diameter [29]. Jiyun Kim et al. successfully fabricated a magnetic polymer microactuator with CNCs (120 nm diameter) inside [21]. X. Cao et al. and S. Qi et al. both fabricated magnetic filament with carbonyl iron particles (CIPs) inside. Particles are both around 5 μm which is much larger than the size limitation of superparamagnetism. But as shown in figure 5a and 5b (red curve), CIPs still shows superparamagnetism behavior [20], [28]. It seems that superparamagnetism may also exist in micro size particles.

2.2.1.b Matrix materials

Matrix material compose the structure of whole scaffold composite and directly contact with cells in OoC. Therefore, its biological property and mechanical property are relevant.

Firstly, matrix needs to be biodegradable which means material can dissolve or physically disappear after functioning in physiological conditions [30]. Cells are

cultured around matrix material and grow to tissue. Finally, tissue remains and scaffold degrade which is realized by biodegrade matrix. Biodegradable material can be categorized through different methods. According to its degradation process, hydrolysis, enzymatic attack, and other process happen in different biodegradable materials. According to material types, degradation also happen in metal, polymer, and other type materials.

Secondly, considering the mechanical requirement of OoC, biodegradable elastomer polymer is a proper option for matrix. Low Young's modulus and high failure strain are two features of elastomer material. Firstly, its high failure strain makes sure that the composite scaffold in OoC can stand large enough reversible strain. Reported by Prof.Richard and his coworkers, the failure strain of a novel elastomer (poly (octamethylene maleate (anhydride) citrate) (POMaC)) reaches 441%. Secondly, in order to successfully culturing tissue in vitro, close match of mechanical property (Young's modulus) between scaffold material and tissue is important. Many tissues are soft and elastic which means that elastomer can be a compatible choose because of its low Young's modulus [31].

2.2.2 Magnetic setup

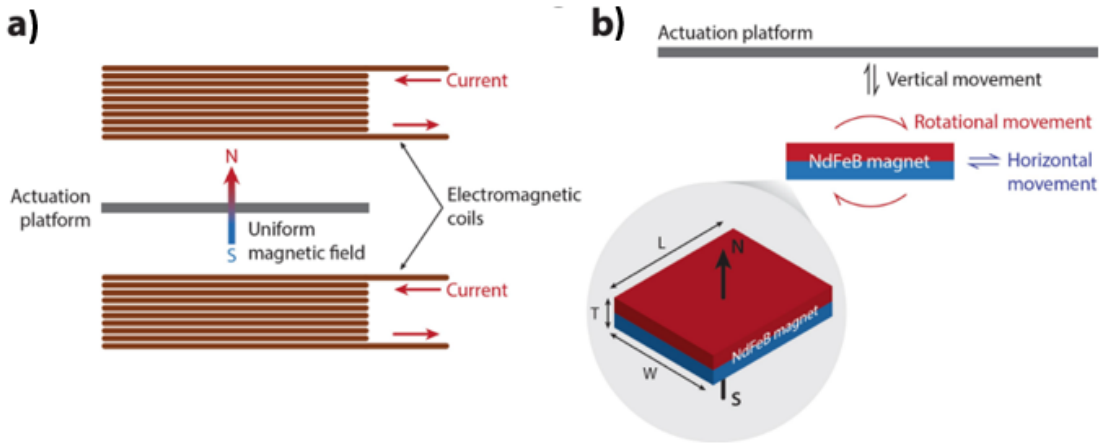

Figure 6. **2 types of magnetic setup used for applying magnetic fields.** a) 2 electromagnetic coils used to generate uniform linear magnetic field. b) Permanent magnet with certain remanent flux density that can generate more complex magnetic field [32].

Magnetic field is needed both for aligning particles during fabrication process and film

actuation which will be illustrated in the following parts. There are two ways to generate magnetic field and control it which are shown in figure 6 [32]. Firstly, uniform magnetic field can be generated through two parallel electromagnetic coils. Particle chains with different orientations can be obtained when film is put on the platform with different tilting angles. For further actuation, opening and closing of current can control the exist of magnetic field which can realize continuous actuation. Permanent magnet is another type of magnetic field source where magnetic field is generated with intensity gradient. However, when the dimension of composite is very small or magnet is very close to it, magnetic field can be regarded as uniform because magnetic force is very small. Different relative position between film and magnet corresponds to different magnetic field. Rotation and movement can both be used to actuation composite film. Field is spatially changing when magnet position is changing.

2.2.3 Magnetic actuation mechanism

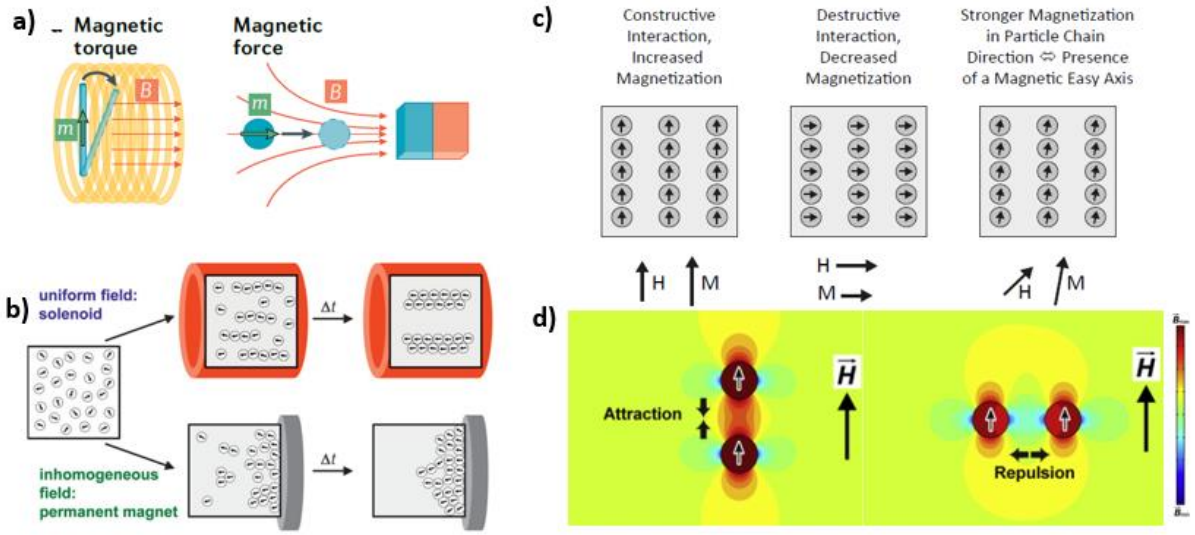

Figure 7. **Magnetic actuation principle of anisotropic magneto-sensitive elastomer film (MSEF) composite filled with magnetic particles.** a) 2 types of interactions between external magnetic field and particle [33]. b) Schematic of magnetic fi eld-directed self-assembly of magnetic particle in uniform and inhomogeneous magnetic field [34]. c) ① Constructive interference between particles due to parallel relation of magnetic field and particle distribution. ② Destructive interference between particles due to perpendicular relation of magnetic field and particle distribution. ③ Magnetization direction is tilted a bit towards particle line due to constructive interference [35]. d) Schematic of attractive and repulsive dipole interaction between 2 magnetic

particles [36].

Firstly, the actuation principle of MSEF filled with particles will be demonstrated. There are two types of forces generated on the particles by external magnetic field which are shown in figure 7a [33]. Magnetic torque tends to rotate the magnetization direction toward the direction of magnetic field so that the Zeeman energy is minimized [37]. Magnetic force is generated only in non-uniform field which is also named magnetic translation force [38]. Its driving force is magnetic field gradient. In non-uniform field, magnetic translation force tends to move magnetic particles toward higher magnetic field position.

Particles distribute differently in uniform and non-uniform magnetic field which is shown in figure 7b [34]. The discussion below is about particle movement in composite fabrication process where all the particles are not fixed and can move in composite matrix. For uniform field, magnetic particles tend to form chains along magnetic field due to magnetic torque on particles and the interaction between particles [21]. As shown in figure 7c, particle interaction is constructive when chains are formed along field direction [35]. 'Constructive' can be explained from two aspects. From magnetization aspect, magnetization of every particle is enhanced which can be found by comparing two figures in figure 7d. From energy aspect, particle interaction energy is minimized when chains are along with the field. The expression of particle-particle interaction energy U is shown in formula (1) [36].

$$U = -(3\times\cos 2\alpha - 1)\times m^2/d^3 \quad (1)$$

α is the angle between magnetic field and connecting line of two particles. m and d are external field induced moment in one particle and distance between two particles respectively. When α is zero (field aligns with chain), particle interaction energy is lowest. Therefore, chains tend to align with field as it is energetically favorable. For non-uniform field, magnetic translation force is also exerted on particles due to field gradient. This translation force tends to move particles toward the strongest field region [35]. For this situation, particle distribution is more complex. Dipolar interaction between particles and magnetic torque tends to align particles toward the chains while

translation magnetic force moves particle toward the surface of film where the magnetic field is strongest. Therefore, when dipolar interaction force dominates the particles tend to form chain-like distribution. When translation force dominates, the particles tend to accumulate near film surface where magnetic field is strongest and increase the particle density there which is shown in figure 7b [26]. Especially for devices with small dimension, sometimes magnetic translation force can be ignored. Zhang et al. [38] fabricated cilia with 50 μm diameter and 350 μm length. Magnetic particles distribute randomly in cilia. Their calculation result shows that magnetic torque is about two orders of magnitude larger than the torque generated by magnetic translation force for small cilia. It may be because that field gradient is very small in small object. Therefore, it is possible that particles align along field lines even in inhomogeneous field because translational force is not dominant.

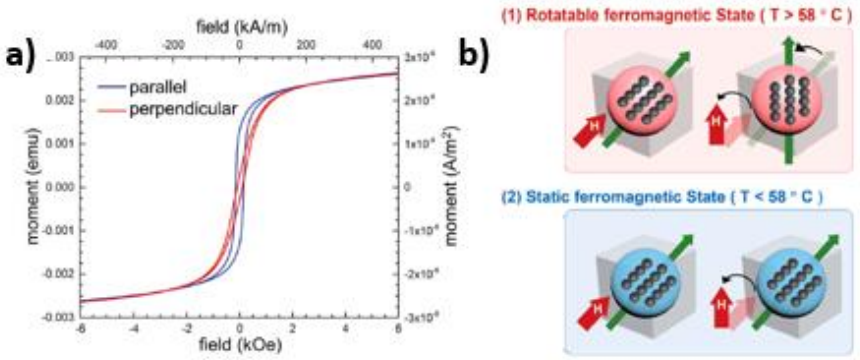

Figure 8. **Introduced magnetic anisotropy of magnetic particle chain.** a) Magnetometry of a chained polymer composite filled with particles when magnetic field parallel and perpendicular to the chain. It is measured at 300 K [37]. b) Rotatable and static ferromagnetic states of magnetic particles [39].

As mentioned above, except interaction between magnetic particle and external magnetic field, magnetized particles also interact with each other which is also named particle interaction or dipolar interaction. From both magnetization and energy aspects, particles alignment tends to be head-to-tail which is constructive. When the alignment is perpendicular to magnetic field, the interaction is destructive. Due to above magnetic interactions, particles present chain-like distribution in uniform magnetic field. This

type of distribution introduces magnetic anisotropy in film which is called particle-alignment induced anisotropy. There are three types of magnetic anisotropy: Magnetocrystalline anisotropy, shape anisotropy and particle-alignment induced anisotropy [35]. In anisotropic MSEF composite filled with magnetic particles, particle alignment induced anisotropy overrides magnetic anisotropy. Mishra et al. [37] fabricated thermoplastic polyurethane composite film filled with Fe_3O_4 particle chains. Magnetometry of film is measured when chains are parallel and perpendicular to the field. The result in figure 8a shows that it is easier to magnetize when chains are parallel with magnetic field and magnetic easy axis is along chain direction. Therefore, it proves that chain introduced anisotropy dominates in the film.

After fabrication, all the particles are fixed in matrix and film is ready for actuation. Magnetic anisotropy is the origin of magnetic actuation. When applied field is not in the same direction as particle chain, particles tend to move and become parallel to field direction [21]. It is because higher magnetization and lower dipolar interaction energy can be achieved when chains are parallel to the field [36]. However, particles cannot move when the composite is already cured or solidified. Besides, the magnetic forces exerted on particles are transferred to film matrix due to interfacial jamming [39]. It is shown in figure 8b, particles cannot rotate or move when they are fixed.

Therefore, film will be deformed when applied field is not in the same direction with chains and try to make chain align with magnetic field as much as possible. This deformation is driven by cooperative magnetic torque induced by chains [21]. After deformation process, film will reach balance state and does not move. Cooperative magnetic torque will become balanced with elastic force of deformed matrix which is the resistance of deformation [28]. Final balance deformation state is reached when magnetic energy plus elastic energy is the lowest.

2.2.4 Fabrication of composite of elastomer and magnetic particles

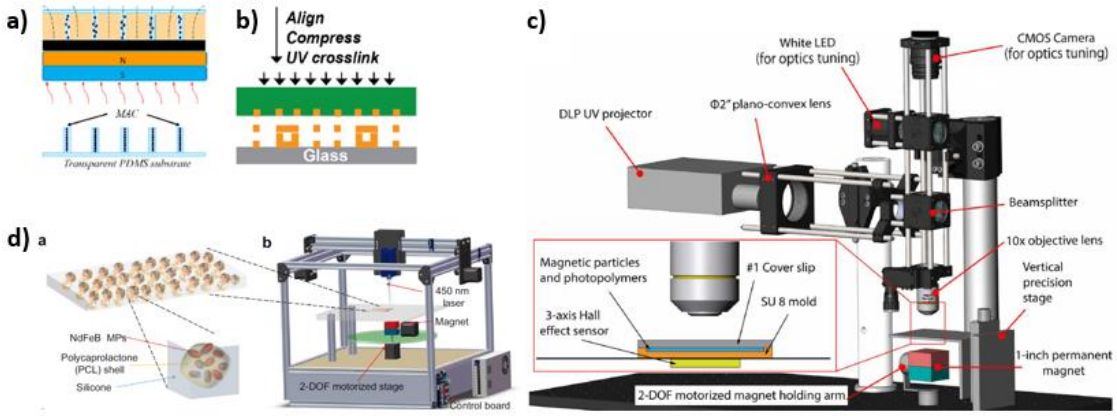

Figure 9. **A few methods used to fabricate polymer composite filled with magnetic particles.** a) PDMS filled with CIPs are cured under 80 ℃ with the magnet aligning particles in PDMS [38]. b) POMaC prepolymer is exposed to UV light for crosslinking [4]. c) Setup that can be used to selectively cure local elastomeric matrix (UV resin) filled with magnetic particles (NdFeB). 250 μm by 250 μm magnetization feature size can be reached [40]. d) Digital laser writing system that can selectively melt phase change polymer (Polycaprolactone) which is used to encapsulate magnetic particels (NdFeB) [41].

There are many ways to fabricate MSEF composite filled with magnetic particles. The first category is about mixing particles with pre-polymer and then cure it. After particles are filled in elastomer, composite is cured or crosslinked with certain energy so that particles can be fixed in matrix. There are two ways to exert the needed energy on composite. In figure 9a and figure 9b, heating and UV light are used respectively to offer the needed energy for polymerization [4], [38]. In these two situations, the whole film is cured simultaneously. In figure 9c, different areas of elastomer film can be selectively cured by small UV light beam. Its resolution can reach 250 μm by 250 μm [40]. More complex magnetization profile can be realized through this type of fabrication method. Except curing polymers, particles distribution can also be fixed through melting and solidifying of matrix. In figure 9d, NdFeB magnetic particles are encapsulated by Polycaprolactone (PCL) whose melting temperature is much lower than silicone matrix and NdFeB particles. Liquid phase and solid phase of PCL are used to realign particle distribution and fixed particle alignment respectively. Laser is used

to selectively melt PCL with 300 μm resolution [41]. One big advantage of this method is that the particle distribution can be reversibly programmed in composite through melting and solidifying processes.

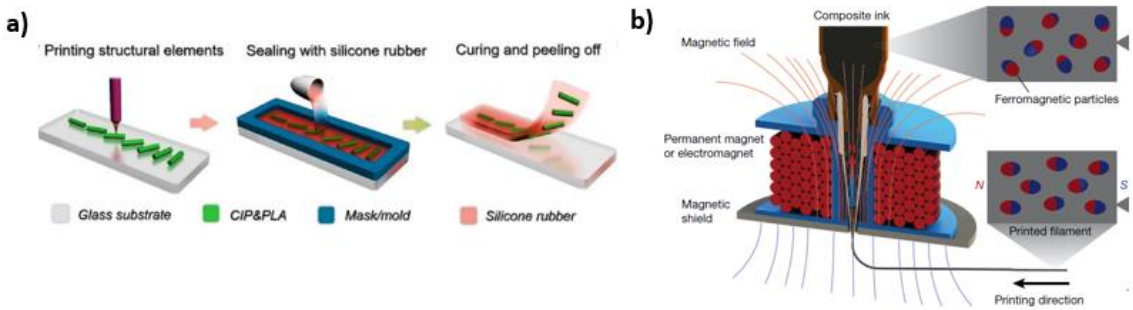

Figure 10. **3D printing that is used for fabricating polymer composite filled with magnetic particles.** a) Schematic of 3D printing structural elements (Polylactic acid (PLA) and CIPs and sealing with matrix material (silicone rubber) [20]. b) 3D printing and reorientation process of silicone filled with NdFeB [32].

3D printing is another effective way to fabricate MSEF filled with magnetic particles. It is a convenient fabrication method for devices with complex structure and magnetization profile. In figure 10a, structural element (CIPs) with different orientations is 3D printed through Fused Deposition Modelling. After printing, it is sealed with matrix material (silicone). The composite film is cured at room temperature [20]. In figure 10b, silicone ink filled with NdFeB particles are 3D printed through direct ink writing. At the same time, particle magnetizations are reoriented through changing magnetic field. By adjusting magnetic field in printing process, complex magnetic profile can be realized. When printing is finished, the printed object is heated under 120 ℃ to solidify [32].

2.2.5 Magnetic actuation methods

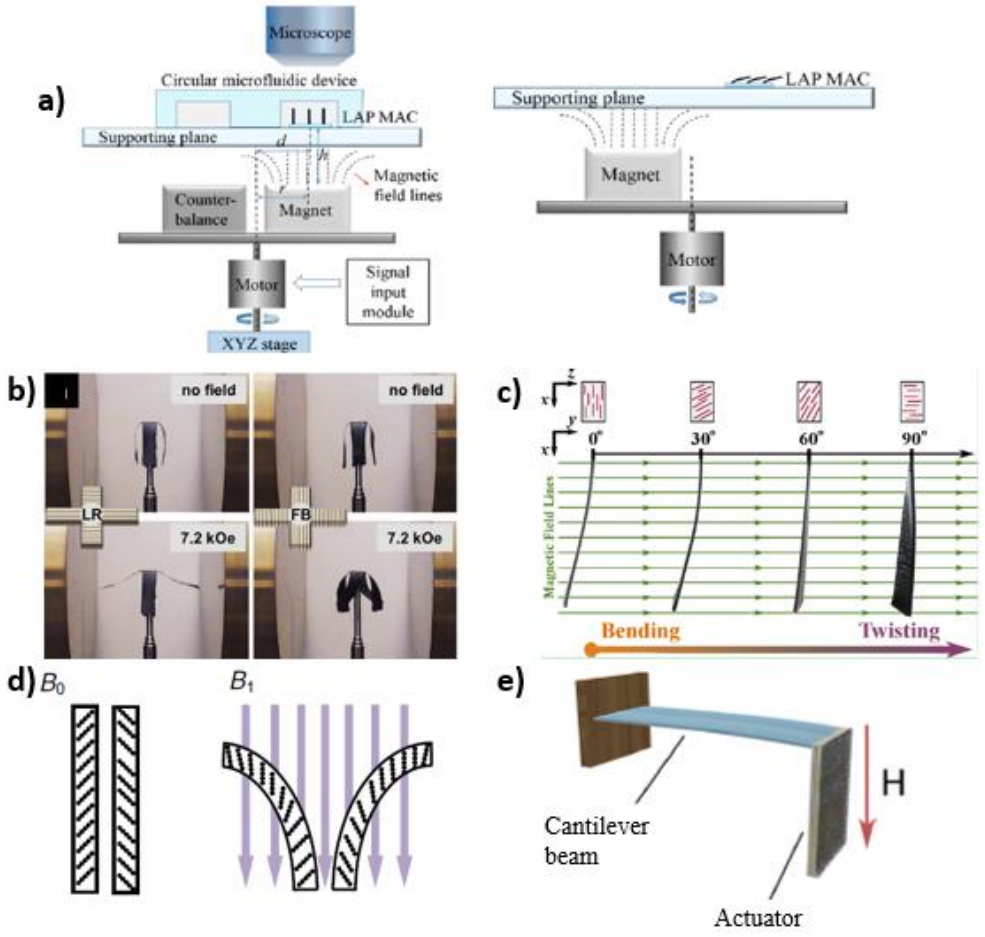

Figure 11. **Bending, twisting, and stretching deformations (bending: a, b, c, d, twisting: b, c, stretching: d, e) of composite elastomers filled with magnetic particles.** a) Schematic drawing of the bending cilia driven by rotating magnet [38]. b) Particles in the device are parallel and perpendicular to the horizontal uniform magnetic field [37]. c) Actuation of composite with different magnetic fiber angles in horizontal uniform magnetic field [42]. d) 2 beams filled with magnetic particle chains along different directions are put in the environment without magnetic field and with vertical magnetic field [43]. e) An actuator filled with homogeneous magnetic particles are fixed at the end of cantilever. Stretching deformation is observed when a perpendicular magnetic field is applied [44].

As discussed before, particle chains tend to align with external magnetic field which is the origin of magnetic deformation. Different actuations can be realized through different chain alignments and external fields. Three types of actuation methods will be demonstrated below. Firstly, bending deformation of elastomer filled with magnetic particles are well researched and there are also a few ways to realize it [37], [38], [42], [43], [45]. In figure 11a, cilia filled with magnetic particles is fabricated and actuated.

Firstly, particles are aligned along longitudinal direction and cured. Then, a rotating field with spatially changing field is used to generate continuous bending actuation. Because chains in cilia tend to align the longitudinal direction with field line [38]. Bending can also be generated through uniform magnetic field. At the left side of figure 11b, particle chains are parallel aligned along horizontal direction. When electromagnetic coil is open, two sides bend upwards. When magnetic field is off, it will return to the original position under gravity effect. Therefore, continuous bending actuation can be realized by switching between opening and closing of coil [37]. Twisting deformation is shown in both figure 11b and figure 11c. At the right side of figure 11b, chains are perpendicularly aligned along horizontal direction. When field is applied, two lateral beams twist in order to make chain align with field line [37]. Bending and twisting are closely related. As shown in figure 11c, bending and twisting are realized when chains are along longitudinal direction and transverse direction respectively. Besides, combined deformation of these two can be generated by tilted chains with certain angle [42]. Except bending and twisting, stretching deformation can be realized in two possible ways. In figure 11e, PDMS filled with homogenously distributed CIPs is fabricated and put in perpendicular magnetic field [44]. Film tends to stretch along field direction so that particles can better align. Besides, the demagnetization energy may be reduced because of elongated shape. The second possible stretching method is to combine two bending films together. As shown in figure 11d, two beams are filled with particle chains along different directions. If two bending beams are bonded together, two opposite bending can be compensated. The only remaining deformation will be stretching.

2.3. Discussion

For the required strain situation for the skeletal muscle cell and myocardium cell, it was shown that mechanical stimulation is beneficial for cell growth. Different cells experience different physiological environment which means that the required strain for better growth may be different. Therefore, it is important to find the proper mechanical stain range for certain cell. For skeletal muscle and myocardium cells,

proper strains for them are investigated by many researchers. Firstly, strain with certain value should benefit cell growth in vitro. Secondly, the strain should not be too large so that the cells will not be damaged. Strain with 15% amplitude is regarded as a proper value for both skeletal muscle cell and myocardium cell according above two rules. Further research is needed for finding the best strain condition for both cells.

In magnetic actuation section, the first small part is an introduction of composite material. Then, actuation mechanism is illustrated where mainly two things are covered, including particles alignment and device actuation. Particle chain is the most important structure feature that contributes to magnetic actuation. Different magnetic field can generate different chain. As mentioned in that part, both uniform and non-uniform field can make the particle move in uncured matrix. Uniform field is the most ideal field for chain formation. Because only magnetic torque is generated on particles which can make clear chain structure. For non-uniform field, magnetic translation force may lead to surface accumulation. But it also depends on how strong the magnetic gradient is and the dimension of device. For small device and small gradient (small enough to assume it is uniform), non-uniform field can also lead to chain formation. For uniform field, it only generates straight-line particle distribution which can be hard to generate complex magnetic profile in device. Non-uniform field is more complex which can make complex particle alignments. Besides, complex movement of magnet also contribute to more types of actuations. Different fabrication methods can be used according to their advantages. It can be very timesaving to cure the entire objects while selective curing can take a lot of time. Complex magnetic profile formation is one advantage of selective curing which can make complex movement and deformation possible. Through encapsulating magnetic particle by the material with low melting point, particle alignment can become reversible. 3D printing is also a good way to make complex profile.

As mentioned in introduction, OoC is used to culture mature cells in vitro. Usually, OoC scaffold is static. However, mechanical stimulation is needed for better growth of cell. Therefore, a new type of OoC scaffold which can generate mechanical stimulation

to cells is preferred. Magnetic actuation is a possible way to control this mechanical stimulation. In the project, CIPs and polymer POMaC will be used for magnetic actuator fabrication. The actuator works as the scaffold that will be used in OoC. A scaffold filled with magnetic particles is investigated including it fabrication, characterization, and actuation.

Stretching is the ideal actuation method that want to be realized for stimulating muscle cell. Firstly, it can generate enough strain (15% amplitude for muscle cell). Secondly, it almost does not have deflection comparing with bending. This is beneficial when cells are cultured in nutrition solution because big deflection may make cells on scaffold leave solution. Thirdly, stretching strain is what used in the mentioned papers related to muscle cells. Therefore, better mimicking of physiological microenvironment may be realized through stretching. 2 bending deformations are shown in figure 11,d which can be utilized to realize stretching deformation. Opposite titling direction of CIP chains means opposite bending directions in magnetic field because CIP chains tend to become align with magnetic field lines. If 2 films with opposite CIP chains are bonded with each other, 2 opposite bending can be compensated. Therefore, only certain stretching is generated when the 2-layer bonded sample experiences homogenous magnetic field. This kind of deformation in 2-layers bonded samples is investigated in the thesis.

3

Experimental detail

3.1. Pre-POMaC synthesis

Pre-POMaC is synthesized according to protocol shown in the appendix. Liquid POMaC is named as pre-POMaC which is kind of pre-polymer. After some condensation reactions, pre-POMaC can be synthesized [31]. Firstly, 1,8 octanediol, citric acid and maleic anhydride are added into flask. 3 hours 140 ℃ heating is applied after 3-time N_2 flush in the setup shown in figure 12 a. Synthesized pre-POMaC is shown in figure 12 b. 1-4, dioxane in figure 12 c is used for dissolving pre-POMaC so that the mixture can be used to separate low- weight POMaC molecule and high-weight POMaC molecule. The mixture is shown in figure 12 d.

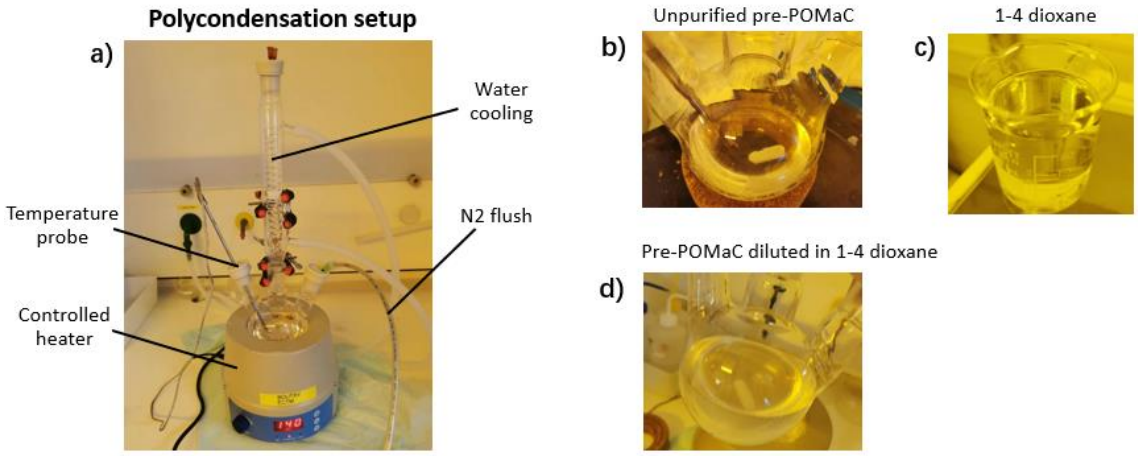

Figure 12. **Pre-POMaC heating synthesis.** a) Polycondensation setup used for synthesizing POMaC. b) Unpurified pre-POMaC which is obtained through 3 hours heating under 140 ℃ in the setup in figure 12 a. c) 1-4 dioxane is used as solvent for dissolving pre-POMaC. d) pre-POMaC solution obtained by pouring 1-4 dioxane in unpurified pre-POMaC. 1-4 dioxane is poured in pre-POMaC when the temperature of POMaC is 100 ℃. Magnetic stirring is applied for 10 minutes for better dissolving.

POMaC/dioxane mixture is poured in separation funnel for purification. Pre-POMaC is collected at the bottom of beaker while unreacted chemicals float on the water surface. After pouring the water out of beaker, the purified POMaC is stored in a new flask shown in figure 13 b. Overnight N_2 flow is applied in order to evaporate all the remaining water and dioxane in pre-POMaC. Finally, transparent pre-POMaC is obtained. More operation details can be found in the appendix.

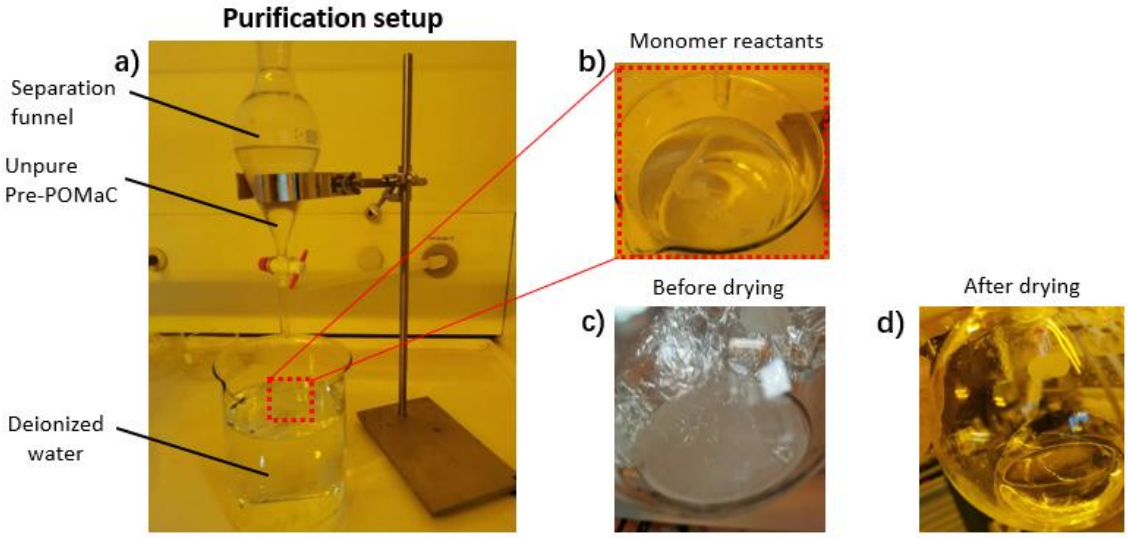

Figure 13. **Pre-POMaC purification and drying process.** a) Purification setup used for separating pre-POMaC (at the bottom of beaker) from monomer and pre-POMaC which are not fully polymerized (on the top of beaker). 2L water is filled in the beaker. b) pre-POMaC obtained at the bottom of beaker is transferred to a new flask. c) N_2 gas flow is applied to pre-POMaC overnight in order to get rid of 1,4-dioxane and water.

3.2. POMaC/CIP film fabrication

The fabrication process of thin film samples is shown in figure 14. Firstly, the thin film layer with certain structure feathers is 3D printed by Sigma and fixed in wafer box for PDMS molding. PDMS is prepared and poured into the single wafer box. After curing PDMS, it is peeled out of the box and bonded with glass slide for POMaC/CIP injection. The injected PDMS mold is curing under UV light. For all the 1-layer pure POMaC and 1-layer POMaC/CIP samples 6-minute UV exposure is applied to each side. Totally, all the 1-layer samples experience 12 minutes UV exposure. Finally, a POMaC layer is obtained after PDMS is uncapped from the glass slid. To fabricate 2-layer sample, 1-layer samples will be bonded with each other through manual alignment operation.

Extra oven curing and /or UV exposure are applied for enhancing the adhesion between 2 layers. Specific bonding parameters vary for different batches of sample. Be careful with the flipping method for POMaC/CIP sample which may influence the CIP chain distribution. More detailed information can be found in the protocol (appendix).

In figure 15, some pictures of certain steps are shown. For all the fabricated POMaC/CIP sample in this thesis, 40% mass percent CIP is add into POMaC. In figure 15 a, orogen/initiator/POMaC/CIP are mixed with each other in the beaker through spatulas. The mixture is put on the hotplate (90 -120 °C) during mixture process. In figure 15 b, the mixture is poured in to syringe and injected into PDMS mold. After that, samples are put on the configuration shown in picture 15 c in order to generate CIP chain distribution inside the composite. The permanent magnet is titled to 45 ° so that 45-degree chain distribution can be realized. Mold filled with POMaC/CIP mixture is exposed to UV light. In figure 15 d, all the demolded samples are transferred to PBS for leaching out all the remaining initiator and porogen as shown.

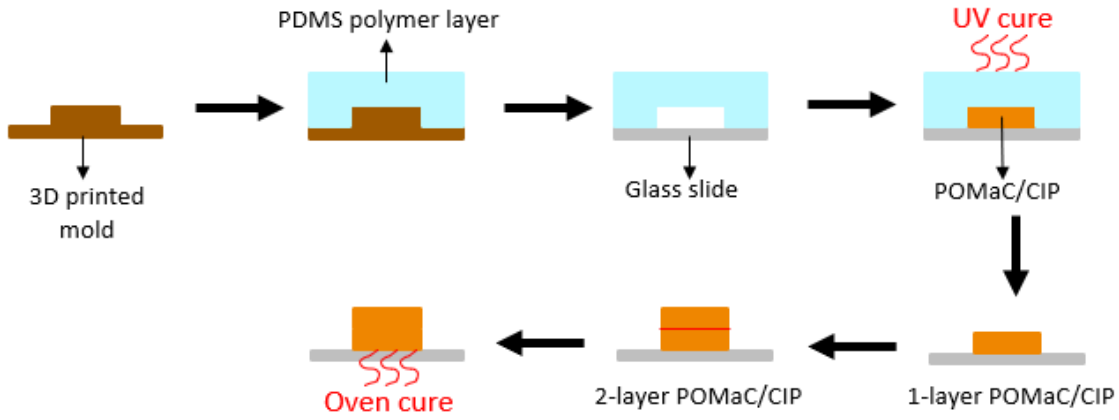

Figure 14. Procedure used for fabricating POMaC and POMaC/CIP samples through PDMS molding and injection. More details are shown in the appendix.

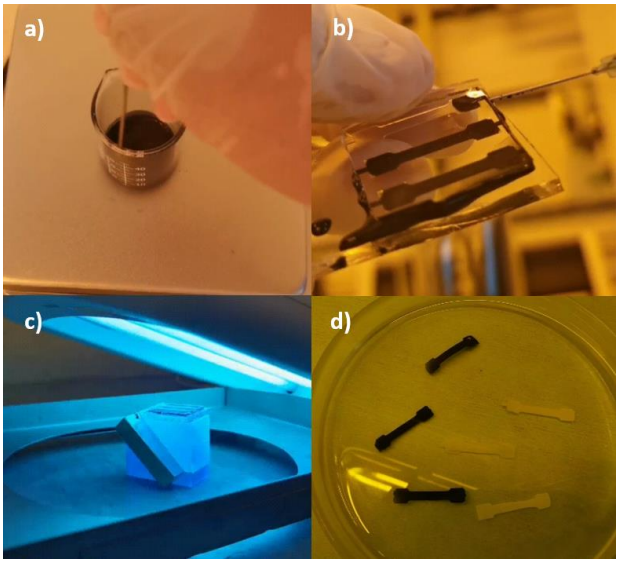

Figure 15. **Procedures needed for pure POMaC and POMaC/CIP sample fabrication.** a) Mixing POMaC, CIP, porogen and initiator in beaker with spatula on the hotplate. b) Injecting POMaC/CIP into PDMA mold. c) UV light exposure to the sample which is applied to magnetic field. d) Leaching porogen and initiator out of sample through PBS solution.

In order to increase the homogeneity, it is important to flip the mold after certain exposure and continue exposure the other side after flipping. Be careful with the flipping method. In figure 16 head ① should be flipped to the position of head ② so that the CIP chain distribution direction is not changed after flipping.

Make sure that the 3D-printed molds are placed on the wafer box flat. Otherwise, the poured PDMS may flow into interface between 3D-printed molds and the bottom of wafer box which makes the obtained PDMS mold tilted. When peeling off PDMS mold layer from wafer box. Only remove the PDMS mold of feature layer and keep the blank PDMS in the box as shown in figure 17.

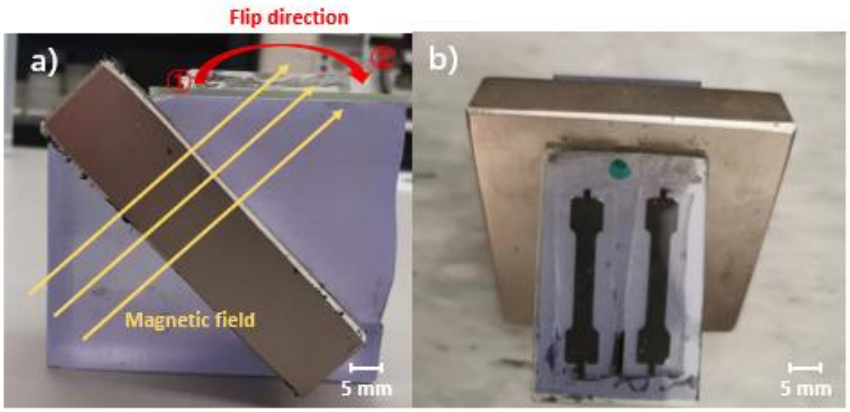

Figure 16. **Configuration used for magnetizing POMaC/CIP samples and generating CIP**

particle distribution. a) Side view. b) Top view.

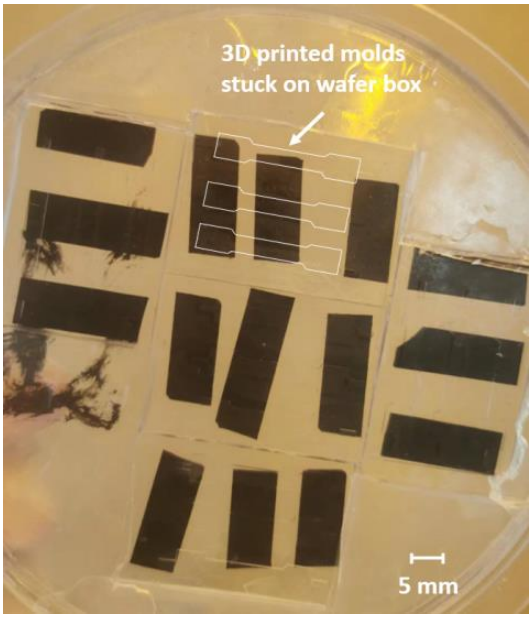

Figure 17. Layout of 3D-printed molds on single wafer box.

3.3. Scanning Electronic Microscopy (SEM)

XL30 SFEG is used for scanning the cross section of POMaC samples where CIP distribution can be observed. Depending on the electron charging situation at surface and needed resolution, the applied voltage ranges from 2 KV to 5 KV. Before measurement, working distance is maintain at 5 mm so that clearer picture can be taken.

3.4. Vibrating Sample Magnetometer (VSM)

VSM is used for measuring the magnetic property of sample. M-H curve can be obtained from the measurement. The working principle of VSM is demonstrate in figure 18. For powder sample, it is encapsulated in a capsule. For thin film sample, it is usually stuck on the sample holder which moves up and down during measurement. External magnetic field is applied by 2 electromagnets which are used for magnetize the sample. The sample holder stuck with sample cuts the magnetic field with a frequency of 40 Hz so that the magnetic field generated by magnetized sample can be transferred to the detected current in pickup coil. Through measuring the current in coil the magnetization of sample is obtained.

As reported in some papers [20], [28], the saturation magnetization of CIP is achieved at around 1 T. Therefore, the range of applied magnetic field is -3 T to 3 T for the

measurement of CIP and POMaC/CIP sample. The step length is 2 second and around 20 mT. The applied magnetic field starts from zero, increase to 3T and falls to -3T. Hysteresis is characterized by the applied cycling magnetic field shown in figure 19.

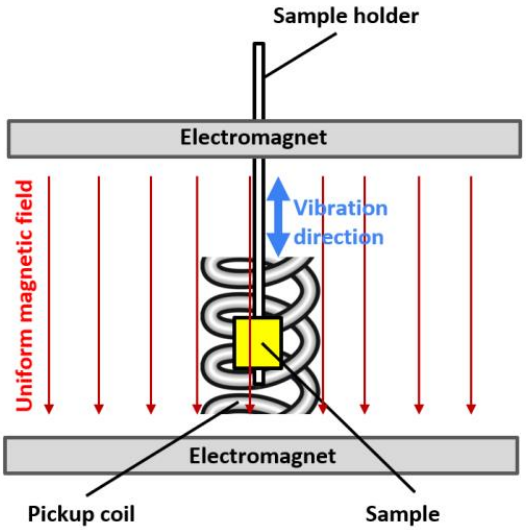

Figure 18. Configuration of Vibrating Sample magnetometer.

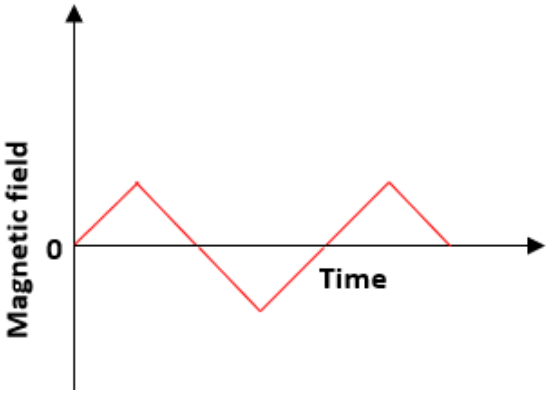

Figure 19. The amplitude and direction of applied magnetic field by electromagnet in VSM.

3.5. Dynamic Mechanical Analysis (DMA)

DMA machine is used for characterizing the mechanical property of POMaC sample and POMaC/CIP sample. Stress-strain curve is measured in 'Strain Rate' mode of DMA. In order to avoid direct contact between the sample and DMA sample clamp which may damage the soft sample. Thin film samples are bonded by double stick and cardboard which perform like a buffer layer of the clamping force [47]. It is also more convenient to load and unload the sample bonded with cardboard. An example of some POMaC/CIP samples bonded with cardboard are shown in figure 20.

Sample is fix in DMA machine as shown in figure 21. 0.1%/s strain rate is used for

measurement [48]. The preloaded force ranges from 0.001 N-000.1 N. Lower preload is applied to softer sample. If the preload is too high, the measurement can not be started as the sample is already stretched before measurement. Proper screw force should be lower than 0.6 N.m which is enough to fix the sample at 2 ends. Otherwise, too high screw force will cause early break close to 2 ends.

Figure 20. POMaC/CIP samples bonded on the paper frame which is made by blade cutter.

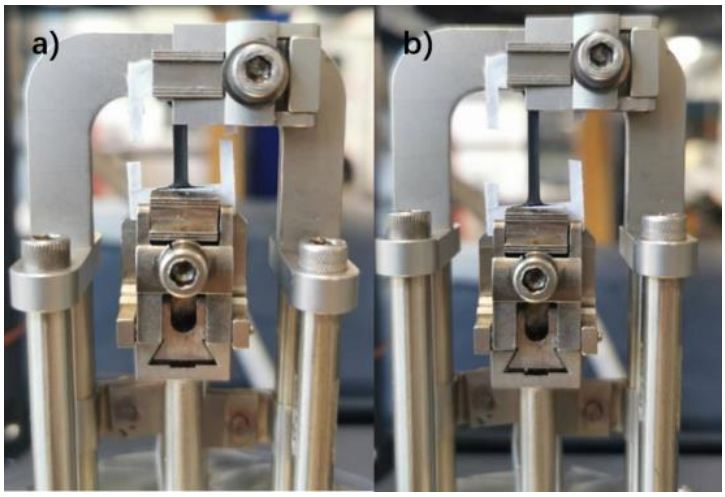

Figure 21. a) Unstretched POMaC/CIP sample fixed in DMA machine. b) Stretched POMaC/CIP sample at around 40% percent elongation.

3.6. Dipole electromagnet

DXSB Air Gap Dipole Electromagnet is used to offer parallel magnetic field for magnetic actuation. HP 6674A is used as the power supply of this electromagnet which can offer enough voltage. The setup shown in figure 22 is used for testing the response of POMaC/CIP sample to magnetic field. The standard working condition for this electromagnet is 60 V/5 A. Both applied voltage and distance between the 2 poles can be adjusted according to the target field intensity. As shown in figure 22, the sample is

stuck on a glass bar and placed at the central part between 2 poles. So that the magnetic field experience by samples is homogeneous and perpendicular.

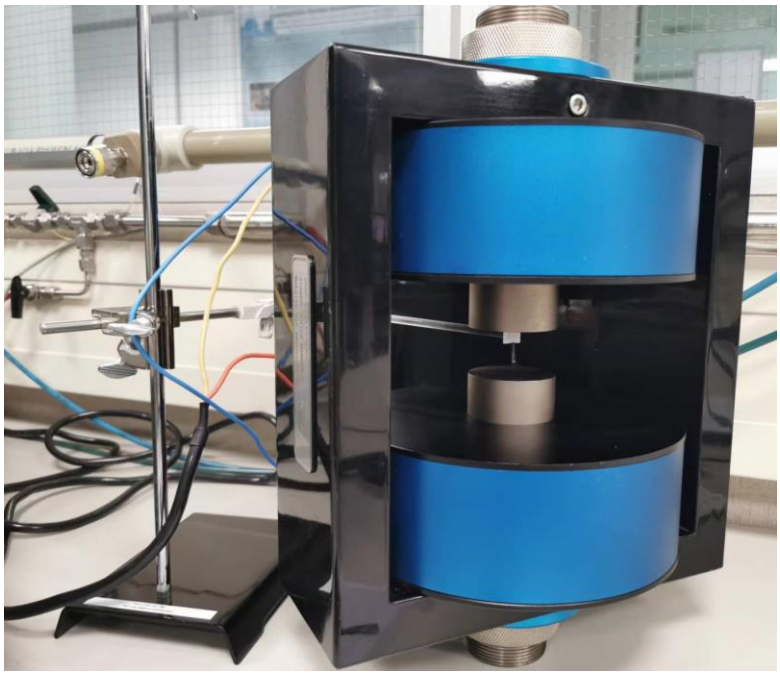

Figure 22. Dipole electromagnet used for actuation and sample holder where POMaC/CIP sample is fixed on it.

3.7. Degradation test

The final application of POMaC/CIP substrate is OoC which will be immersed in PBS solution for culturing the cells. PBS solution is used to mimic the chemical environment inside human body. Therefore, how the properties of substrate change with degradation time is crucial. Both pure POMaC and POMaC/CIP sample are fabricated for PBS degradation test. Mechanical property (Young's modulus), mass and dimension are 3 indicators that are concerned. For pure POMaC and POMaC/CIP, 3 rounds of test will be carried out. Firstly, the properties of pure POMaC and POMaC/CIP samples are measured before being immersed in PBS which is referred as 'Week 0'. The properties are regularly measured after 7 days and 14 days degradation in 37 ℃ PBS solution. The measured samples are referred as 'Week 1' and 'Week 2'. PBS solution in beakers is replaced every week so that the fresh PBS environment is offered.

All the pure POMaC sample and POMaC/CIP samples are fabricated at the same time. The properties of samples which are not immerse in PBS are measured immediately

after fabrication. After that, the remaining samples are put into a beaker filled with PBS as shown in figure 23 a. The lid is closed and the samples are transferred into the incubator (37 °C) as shown in figure 23 b.

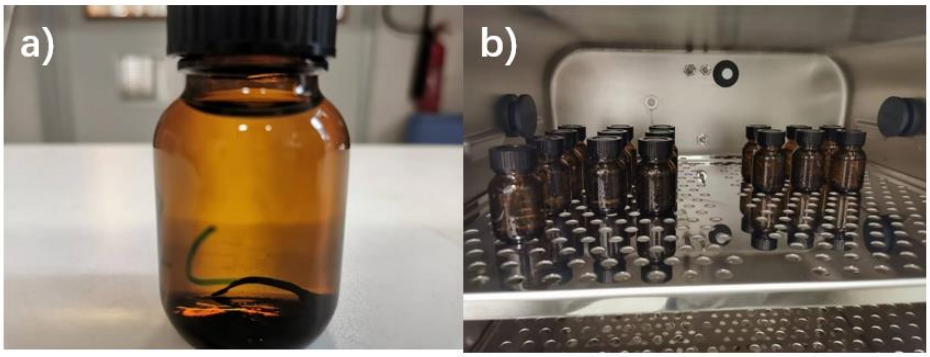

Figure 23. a) POMaC/CIP is immersed in PBS solution in a beaker with closed lid. b) POMaC and POMaC/CIP samples immersed in PBS solution are incubated in the incubator at 37 °C.

4

Result and discussion

4.1. Material characterization

4.1.1. Pre-POMaC

Pre-POMaC is synthesized through the procedure described in section 3.1. and the protocol in appendix. Pre-POMaC refers to the pre-polymer which are synthesized by some condensation reactions among 1,8 octanediol, citric acid and maleic anhydride. After synthesis and purification, overnight N_2 drying is applied to pre-POMaC. It looks transparent and viscous as shown in figure 24 which are features of POMaC [46]. Two batches of pre-POMaC are synthesized. The density of the batches is 1.06 g/cm^3 and 1.11 g/cm^3. For the pre-POMaC 'batch 1', after 3 hours heating it is taken out of the heater to cool down until it goes to 100 ℃. For pre-POMaC 'batch 2', it is cooled down with heater until it goes to 100 ℃ which means that longer heat treatment is applied. As shown in figure 40, the mechanical property (Young's modulus) of batch-1 POMaC and batch-2 differentiates. Therefore, pre-POMaC is very sensitive with the heating time which may influence its mechanical property. For both batches of POMaC, the density accords with the value published in the first paper about POMaC [31]. From this aspect, it indicates successful synthesis of POMaC.

Figure 24. Purified transparent POMaC after overnight N_2 drying

4.1.2. Carbonyl iron

Carbonyl iron particle (CIP) is purchased from Sigma. In order to better understand the diameter distribution of CIP, SEM is done on CIP. CIP with different diameters can be seen in figure 25. The diameter distribution is obtained from figure 25 by measuring the diameter value one by one. Result is shown in figure 26. As the distribution is not symmetrical, log-normal fitting is used. Most particles range from 1.5 μm – 2.5 μm which is what we need for paramagnetic property [35].

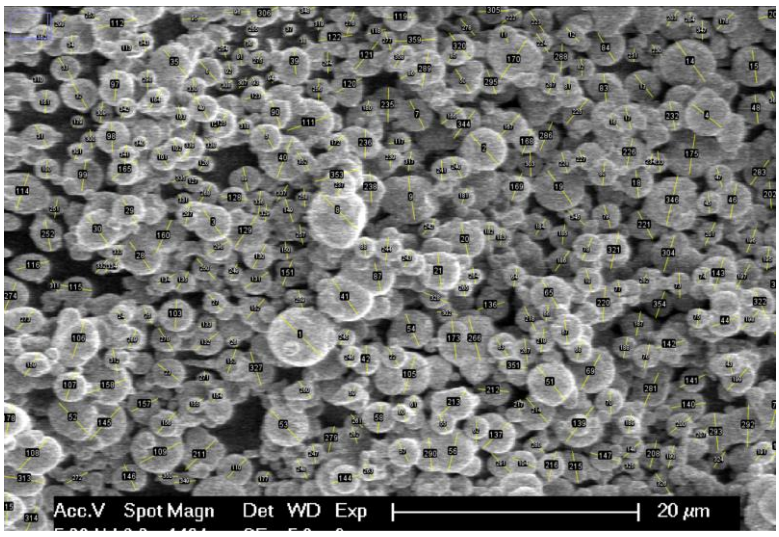

Figure 25. SEM image of CIP with markers for diameter measurement.

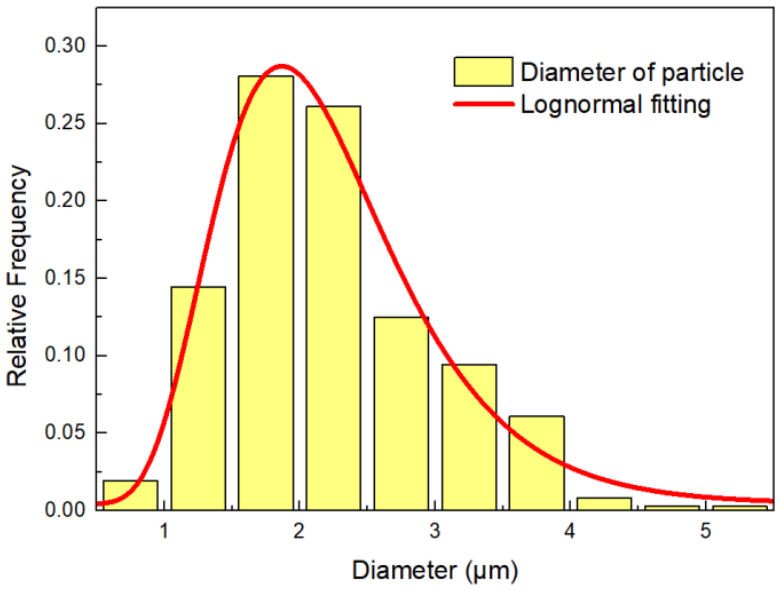

Figure 26. Diameter distribution of the CIP particles and corresponding lognormal fitting (calculated basing on figure 25).

Magnetic property of CIP is characterized through VSM at two different temperatures. 310 K is the working temperature of organ-on-chip. 3.65 mg CIP is accommodated in a capsule for measurement. The saturation magnetization of CIP reaches 0.000752 Am^2 and 0.000750 Am^2 at 298 K and 310 K for 3.65 mg CIP respectively which corresponds to 206 Am^2/kg and 205 Am^2/kg. The results (M-H) curves are shown in figure 26 and accord with the value measured in [20]. High saturation magnetic moment can contribute to stronger magnetic response of sample to the magnetic field. CIP shows small residual magnetization which indicate good paramagnetic property of this material. Low residual magnetization is good for homogeneous distribution of CIP in POMaC during the mixing process [35]. There is almost no difference between curves measured at 310 K and 298 K. It can be explained by high Curie temperature of iron. Such a small temperature change can hardly lead to a property change.

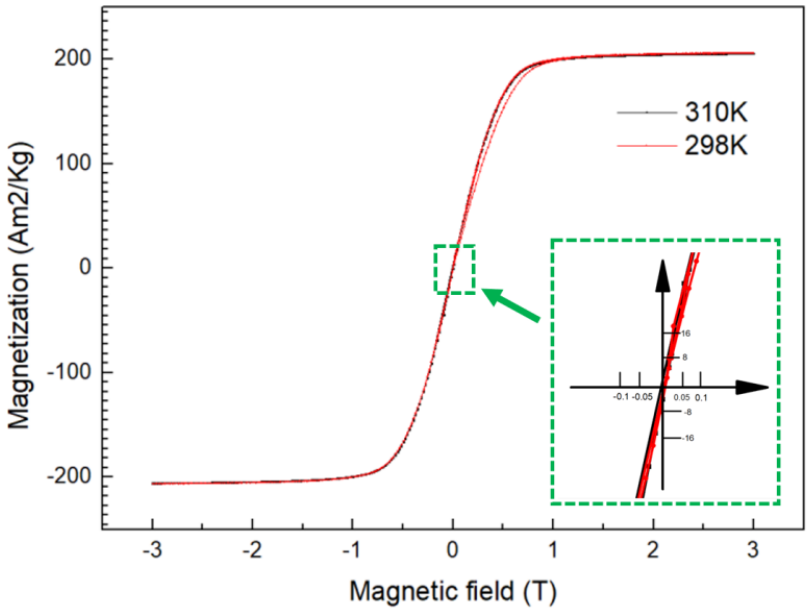

Figure 27. Magnetic property of CIP measured at 310 K and 298 K.

4.2. Film characterization

4.2.1. Film structure

Planar structure of scaffold thin film is shown in figure 29. The thickness of it is 0.3 mm which is a reasonable thickness for OoC application [4]. Dumbbell shape sample is designed for scaffold fabrication. The reasons are as follows: 1- Dumbbell sample can be directly used for tensile test. 2- two heads of it are used for magnetic property measurement. 3- two dumbbell samples can be bonded together for final actuation test. Therefore, all the samples can be fabricated based on one structure which can make the measurement results consistent. In the following parts, all the samples are fabricated through the structure in figure 29. 1-layer sample refers to the single layer sample fabricated from the mold in figure 28. 2-layer sample refers to two 2 1-layer samples that are stacked and bonded together which are shown in figure 28 b. The final functionality of the composite substrate that we want to achieve is to offer stretching deformation through 2-layer POMaC/CIP sample in magnetic field. As shown in figure 28 a, two 1-layre samples bend toward the magnetic field line direction when perpendicular magnetic field is applied. It is because the magnetic energy is minimized

when chains and filed lines are aligned. Two 1-layer samples are bonded with each other in figure 28 b in order to compensate the deflection in two opposite directions. Therefore, when magnetic field is applied only certain stretching deformation remains.

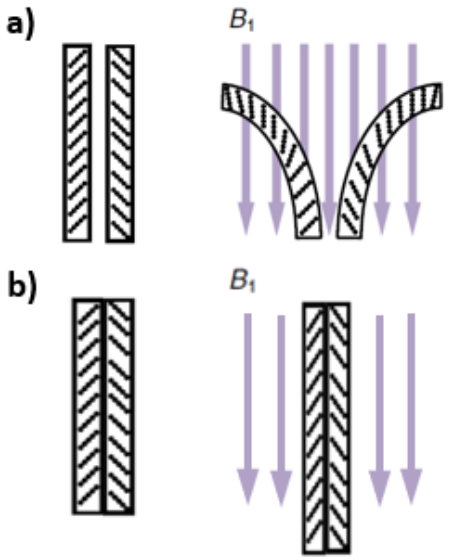

Figure 28. Deformation mechanism of a) 1-layer POMaC/CIP sample. b) 2-layer POMaC/CIP sample.

All the samples are fabricated according to the description in section 3.2. and details in the protocol. After solidification of POMaC/CIP samples, they are immersed in PBS solution for the leaching out of porogen and initiator. In order to check the effectivity of PBS leaching out, 6 pure POMaC samples and 6 POMaC/CIP (40%) samples are fabricated based on the structure in figure 29. The average mass of them are 24.8 mg (± 1.00 mg) and 39.6 mg (± 1.22 mg) respectively where the mass of pure POMaC is 62.6% of POMaC/CIP. The mass of pure POMaC is close to 60.0% of POMaC/CIP which means that most of the remaining porogen and initiator can be leached out of samples through overnight PBS immersion.

Theoretically, 45-degree particle chain distribution will be generated in the thin film with respect to the 45 tilted magnet setup in figure 16. In [49], it is found that the specific magnetic torque value is highest when the angle between magnetic field and particle chain is 45 °. Specific magnetic torque refers to the torque per unit mass divided by the applied magnetic field. Higher specific magnetic torque can lead to stronger

magnetic response. This is the main reason why 45 ° CIP is generated in the matrix. Particle distribution situation is characterized by SEM. As shown in figure 30, the cross-section of thin film is exposed for SEM measurement. Sample is cut to 3 parts because it is too long to be accommodated on the stage. In figure 31 a, a representative example of CIP distribution in POMaC/CIP sample is presented where obvious chain distribution can be seen. 22 SEM pictures are taken in order to record the tilting situation of CIP. 1 SEM presents the CIP distribution situation at 1 position. As shown in figure 31 b and c, from position 1 to position 22, the exposed area is getting further from the magnet. Based on the SEM picture at every position, the tilting angles of CIP chains are calculated. In figure 31 d, tilting angles of chains at different places (from 1 to 22) are shown where the average tilting angle along the whole sample is 35.69 °. From the fitting result in figur31 d, increasing trend of tilting angle is obtained with increasing distance between magnet and POMaC/CIP sample. It may result from the inhomogeneity of magnetic field.

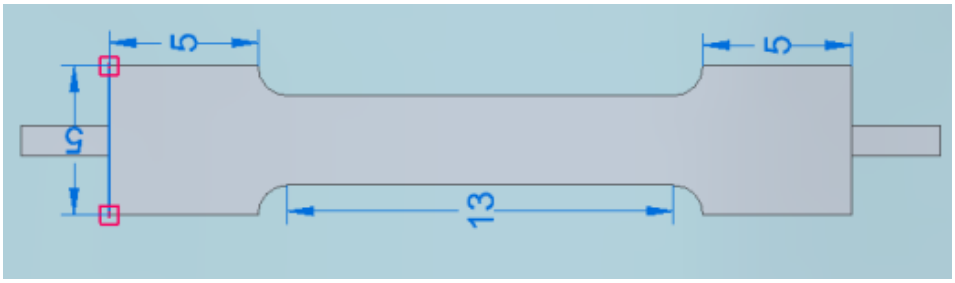

Figure 29. The planar structure of thin film. Unit is mm.

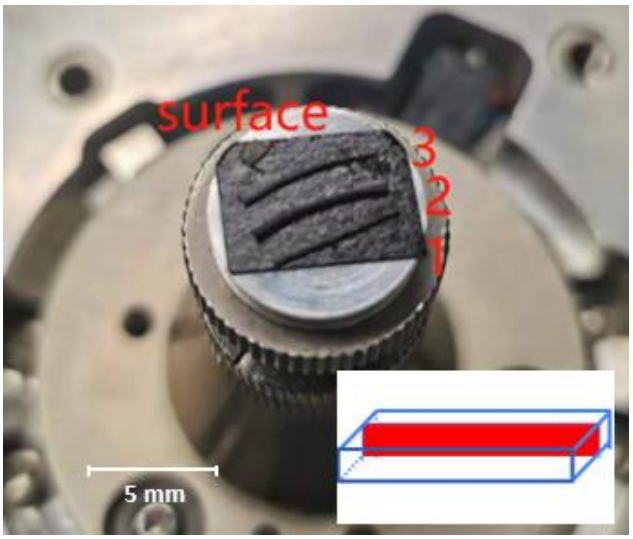

Figure 30. The cross-section of thin film which is stuck on the SEM stage.

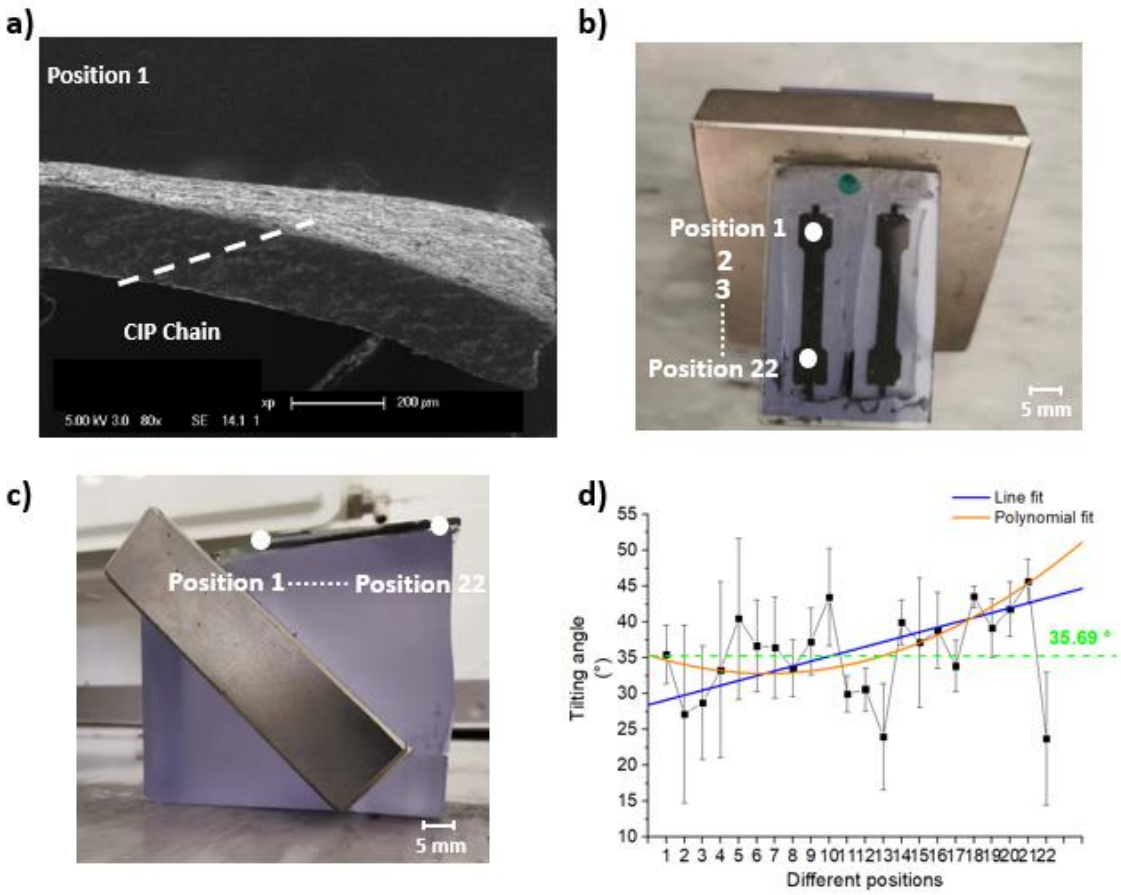

Figure 31. **SEM results and analysis of CIP chains inside POMaC/CIP cross-section.** a) SEM of POMaC/CIP cross-section. b) Measured tilting angle of CIP chain at 22 different positions and corresponding fitting. c) Image of POMaC/CIP sample placed on the magnet setup. d) The relationship between tilting angle and sample position.

2-layer bonded sample is fabricated through aligning and bonding 2 1-layer samples together. Clear opposite chain distribution directions can be found in figure 32 b. For sample shown in figure 32 a, it is directly bonded by 2 layers without oven baking where obvious interface of 2 layers can be observed. In figure 32 b, 1 hour 80 ℃ oven baking is applied to the bonded sample. There is almost no interface which indirectly indicates the formation of chemical bonding between 2 layers. In figure 33, small pores are obtained at the surface of POMaC/CIP sample. It is a crucial structure for nutrient transportation in OoC application. Its size and shape look like what is observed in pure POMaC [4].

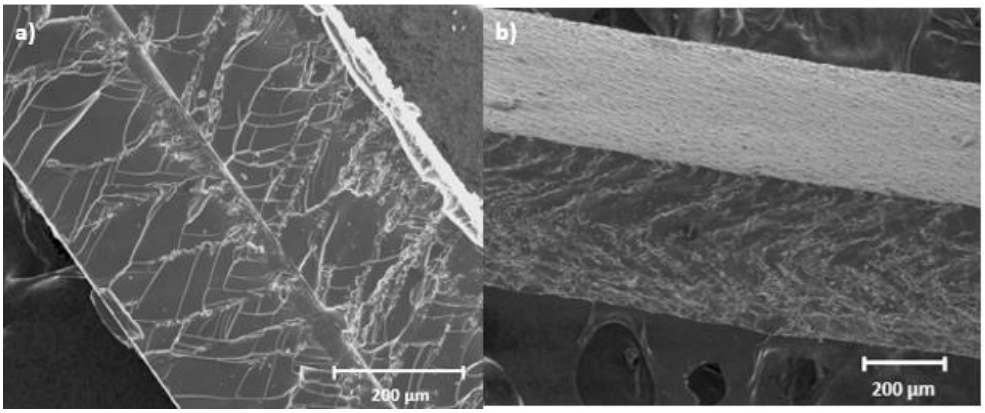

Figure 32. **SEM result of 2-layer bonded POMaC/CIP thin films.** a) Without baking, b) With 1 hour baking at 80 ℃

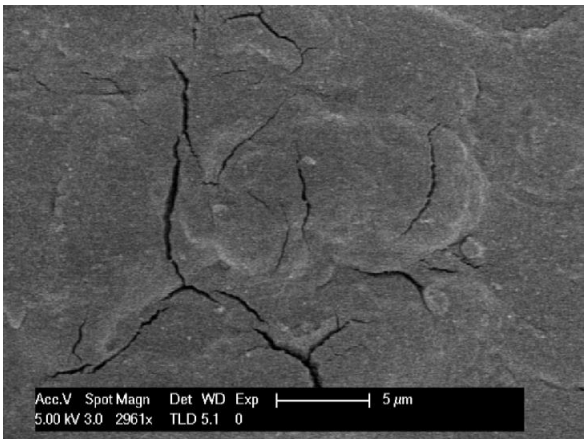

Figure 33. SEM of 1-layer POMaC/CIP sample where small pores are generated on the surface.

4.2.2. Magnetic property

Magnetic property of POMaC/CIP is characterized by VSM. Measurement sample is obtained from the 2 heads of the sample in figure 28. For single layer sample, size is 5 mm by 5 mm with 0.3 mm thickness. The measurement result is shown in figure 34 a. Its saturation magnetization is 72.2 Am^2/kg and 72.0 Am^2/kg respectively at 300 K and 310 K which should be enough for bending actuation according to the other CIP composite elastomer used for magnetic actuation [28], [49]. Besides, it also shows ignorable remaining magnetization. Strong saturation magnetization at 310 K proves the possibility to work under the working temperature of OoC (310 K). For 2-layer sample, its length and width are the same as the 1-layer sample while the thickness is twice as much as the 1-layer one. The measured saturation magnetizations at 300 K and 310 K are 75.8 Am^2/kg and 73.3 Am^2/kg respectively. Higher magnetization at lower

temperature is expected which may be caused by less intense motion of atoms.

Specific operation and details about VSM measurement are explained in section 3.5. Both 1-layer and 2-layer samples are stuck on the holder of VSM so that the magnetic composite film can move with it and show magnetization. There is certain magnetic anisotropy in POMaC/CIP film. Therefore, the magnetization direction is important which show be the same as the applied magnetic field direction during OoC application. As shown in figure 34 c and d, the magnetization directions of both 1-layer and 2-layer POMaC/CIP films in VSM measurement are marked. It is along the longitude direction of POMaC/CIP film.

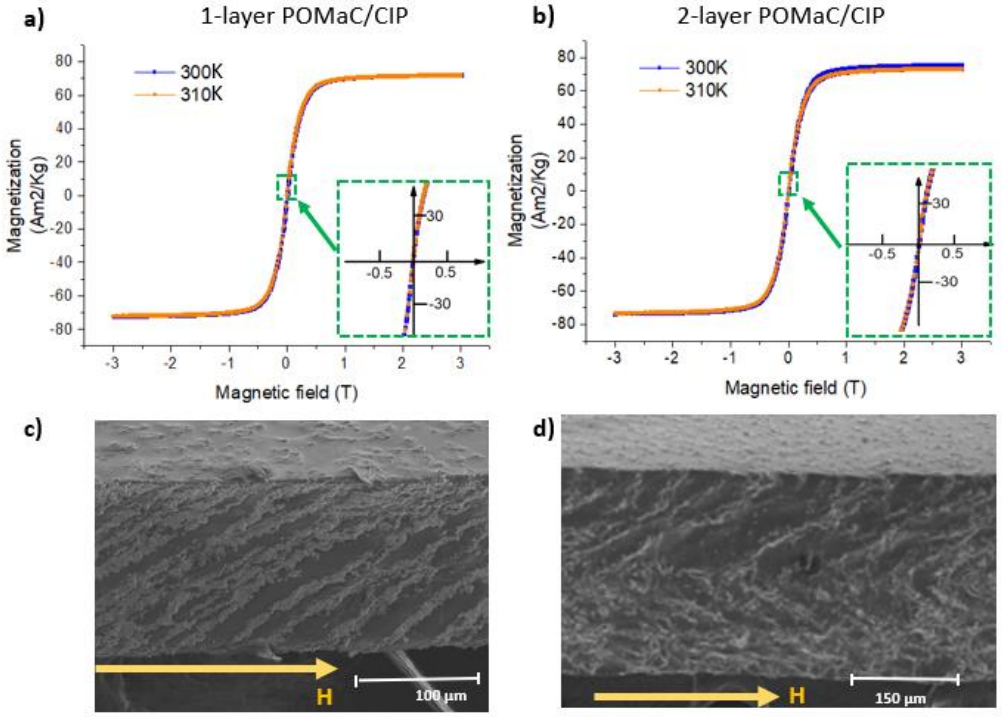

Figure 34**. Magnetic property of POMaC/CIP thin film measured at 310 K and 298 K.** a) M-H curve of 1-layer POMaC/CIP sample. b) M-H curve of 2-layer POMaC/CIP sample c) SEM of 1-layer POMaC/CIP sample with applied magnetic field during M-H measurement. d) SEM of 2-layer POMaC/CIP sample with applied magnetic field during M-H measurement.

4.2.3. Mechanical property

Mechanical property of both pure POMaC and POMaC/CIP is measured by DMA. Specific parameters during DMA measurement are shown in section 3.5. 3 factors that influence the mechanical property of POMaC samples are discussed in this section.

Firstly, the mechanical property of 1-layer and 2-layer bonded samples are compared.

Both pure POMaC samples and POMaC/CIP samples are included. In order to fabricate 2-layer samples, 2 1-layer POMaC samples are bonded together manually and cured under certain condition (eg. UV curing and oven curing) so that the adhesion between 2 layers is sufficient for actuation. Mechanical property of 2-layer bonded POMaC samples is influenced by the curing condition used to bond 2 layers. In figure 35 a and 34 b, mechanical behavior of pure POMaC samples treated with different curing conditions show big difference. Longer heating and additional UV curing increase the Young's modulus of bonded sample although good adhesion can be offered. Then, curing time is reduced to 1 hour in order to keep the elastic feature while bond 2 layers effectively. As shown in the strain-stress curves in figure 35 b and figure 35 c, 1 hour 80 ℃ curing does not have obvious influence on mechanical behavior. Besides, good bonding between 2 layers is obtained after 1 hours curing which is shown in figure 35 d and figure 32 b. It means 1 hours 80 ℃ is suitable for bonding 2 layers pure POMaC and POMaC/CIP without significantly reducing the Young's modulus.

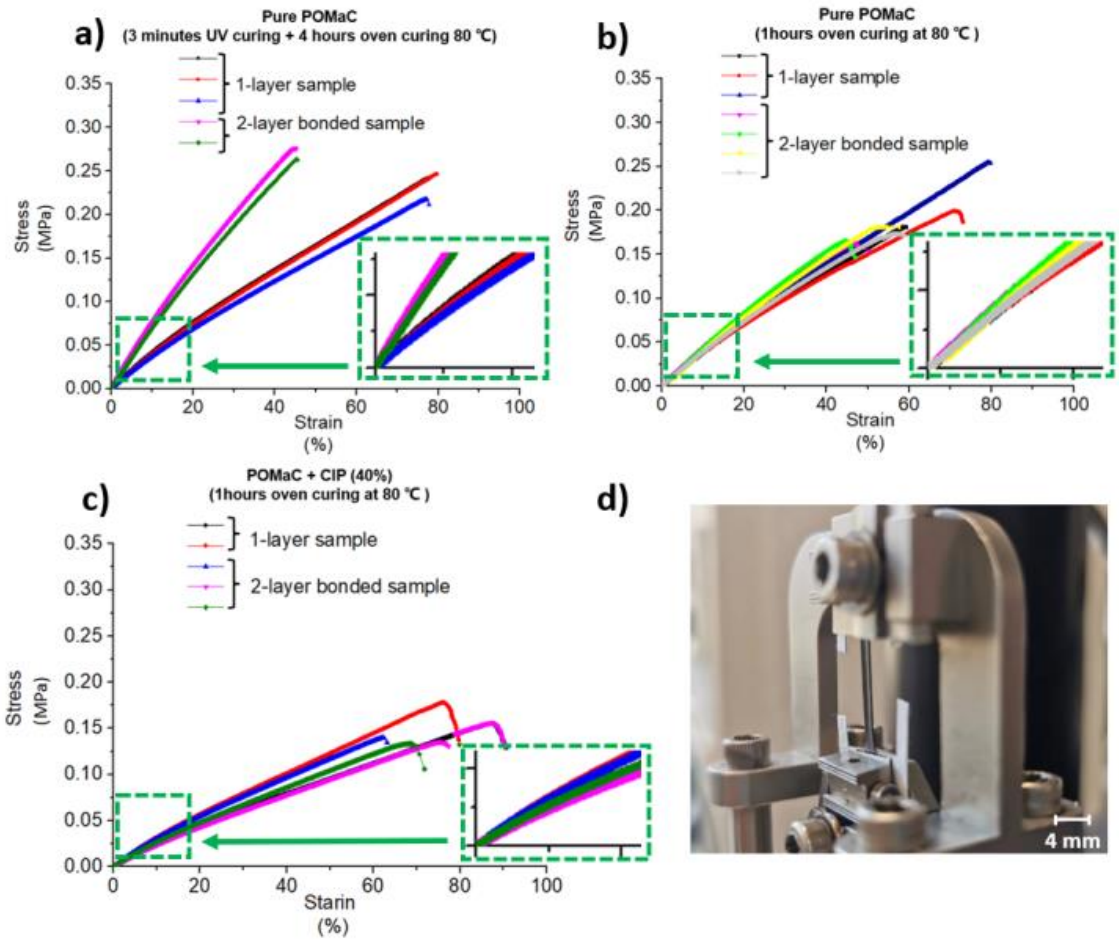

Figure 35. **Influence of bonding condition on mechanical property.** a) Stress-strain curves of single layer pure POMaC sample and bonded 2-layer POMaC sample which is bonded through 3-minute UV exposure and 4 hours baking at 80 ℃. b) Stress-strain curves of single layer pure POMaC sample and bonded 2-layer POMaC sample which is bonded through 1 hour baking at 80 ℃. c) Stress-strain curves of single layer POMaC/CIP sample and bonded 2-layer POMaC/CIP sample which is bonded through 1 hours baking at 80 ℃. d) Stretched 2-layer POMaC/CIP which is curing through 1 hour baking at 80 ℃.

Based on the results in figure 35, Young's modulus in 1-3% and 11-13% are both calculated. Specific values can be found in table 3. It is because the strain range of magnetic stretching goes to maximum 15% for OoC application in order to offer suitable stimulation to the muscle cells as discussed in section 1. Young's modulus lower than 15% is the focus and the magnification of the curves in 0-20% strain range are shown in figure 35. It can be observed from the magnified areas of curves that the gradients of curves decrease with increasing strain. For all the samples shown in table 3, calculated Young's modulus from 11-13% is always lower than 1-3% which mean that the sample becomes softer with increasing strain. It proves the elastomer feature of POMaC and POMaC/CIP samples. It also accords the results in [47].

As shown in figure 36, 4 hours oven curing + 3 minutes UV curing increases the Young's modulus significantly. Theoretically, Young's modulus should increase after 1 hour curing because ester chemical bonding is generated in POMaC [31]. 1-hour curing at 80 ℃ increase the Young's modulus slightly comparing with 4 hours oven curing + 3 minutes UV curing which means that the mechanical property of POMaC is related to the curing condition. The Young's modulus values of pure POMaC samples are within the obtained range in [4].

In figure 37, there is slight decrease of Young's modulus in 1%-3% range although the decreasing value is within the range of error bar. Theoretically, increase of Young's modulus should be observed in figure 37 after 1 hour 80 heating. However, there is almost no obvious change comparing with the 2% and 18% increase of pure POMaC after 1 hour oven curing in figure 36. Perhaps, CIP inside POMaC matrix hindered the formation of ester bonding in heating process so that Young's modulus does not increase that much comparing with pure POMaC. The fabricated POMaC/CIP is elastic enough

for OoC scaffold application. The suitable scaffold should closely match the mechanical property (Young's modulus) of natural tissue. For example, the Young's modulus of cardiac tissue and nervous tissue is 0.9 MPa to 0.2 MPa which are both close to the Young's modulus of fabricated POMaC/CIP [31]. Additionally, the Young's modulus can be further tuned by fabricating parameters if closes match between scaffold and tissue needs be realized.

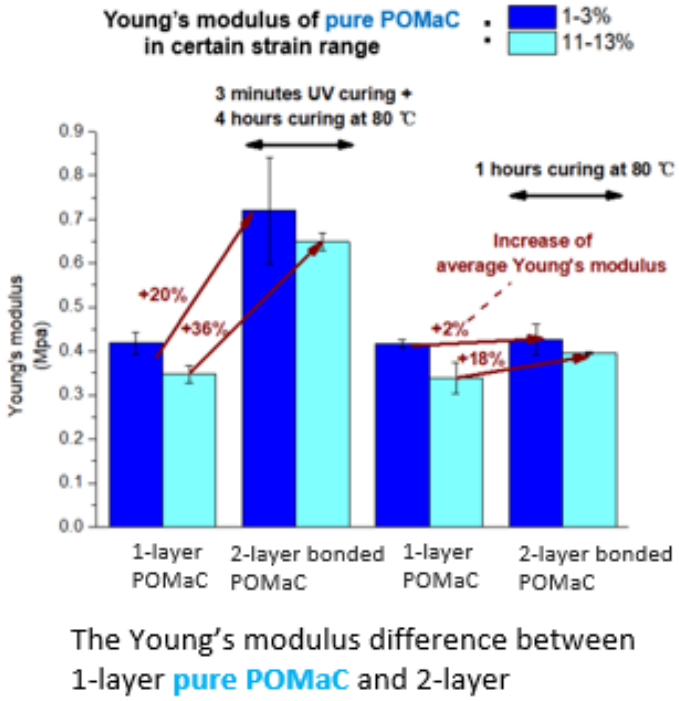

Figure 36. The Young's modulus difference between 1-layer POMaC and 2-layer POMaC which is treated with different conditions.

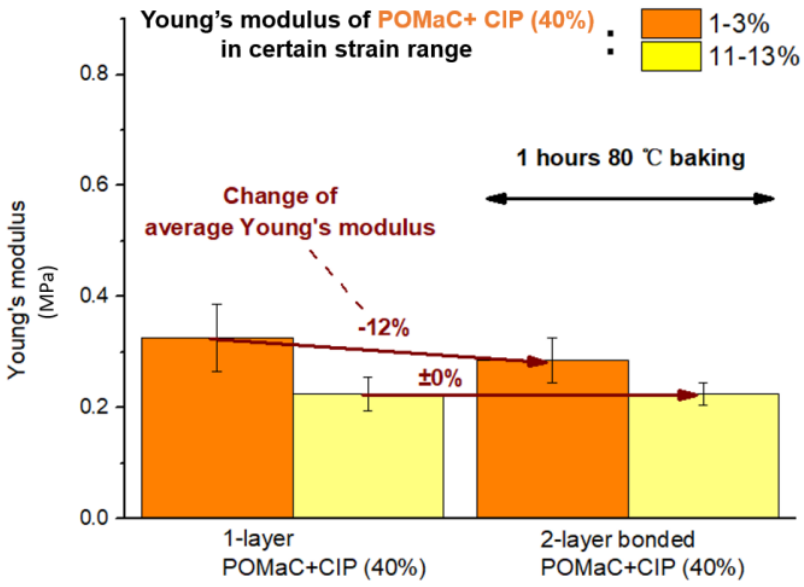

Figure 37. The Young's modulus difference between 1-layer POMaC/CIP and 2-POMaC/CIP.

CIP also plays a crucial role in mechanical property. For both 1-layer sample and 2-layer sample cured at 80 ℃ for 1 hour, POMaC/CIP samples show lower Young's modulus than the pure POMaC in figure 38. For composite material, it usually shows higher Young's modulus than matrix material as the interface between reinforcement elements and matrix material hinders the deformation [50]. Theoretically, POMaC/CIP sample should show higher Young's modulus than POMaC sample if they are fabricated under the same condition. However, the measurement results are opposite. Less polymerization under UV exposure caused by the shielding effect of CIP may be the reason why POMaC/CIP samples show low Young's modulus.

As discussed above, CIP may shield UV light during exposure process when fabricating the 1-layer samples. In figure 39, 2-layer POMaC/CIP sample shows higher Young's modulus comparing with2-layer pure POMaC when the samples are bonded through longer oven curing (80 ℃ 1 hour + 60 ℃ 3 hours). Longer oven curing may effectively cures the shielded parts through ester bonding so that POMaC/CIP shows higher Young's modulus than pure POMaC because of the effect of reinforcement phase (CIP).

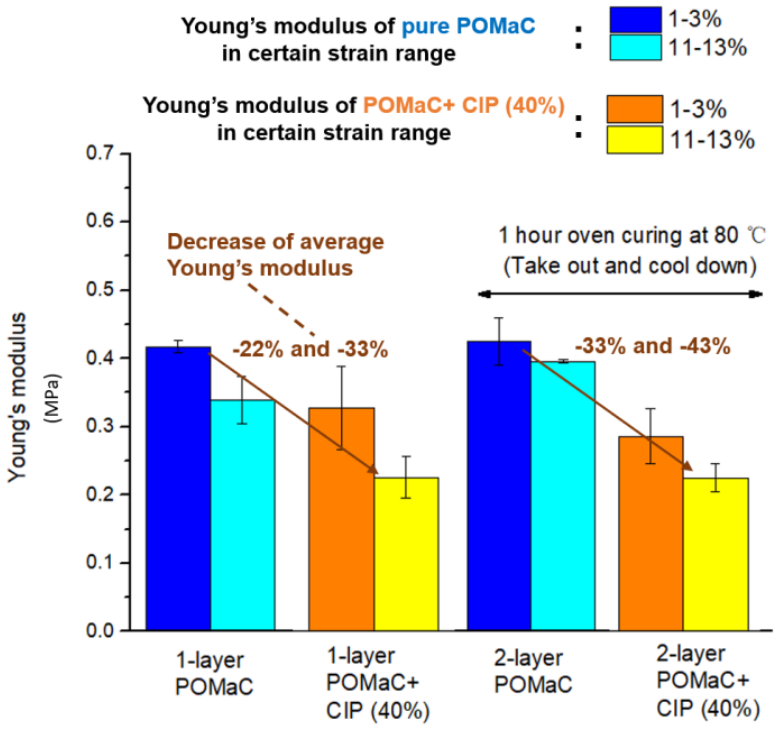

Figure 38. Mechanical property (Young's modulus) difference between POMaC samples and POMaC/CIP samples. Both 1-layer samples and 2-layer bonded samples are compared.

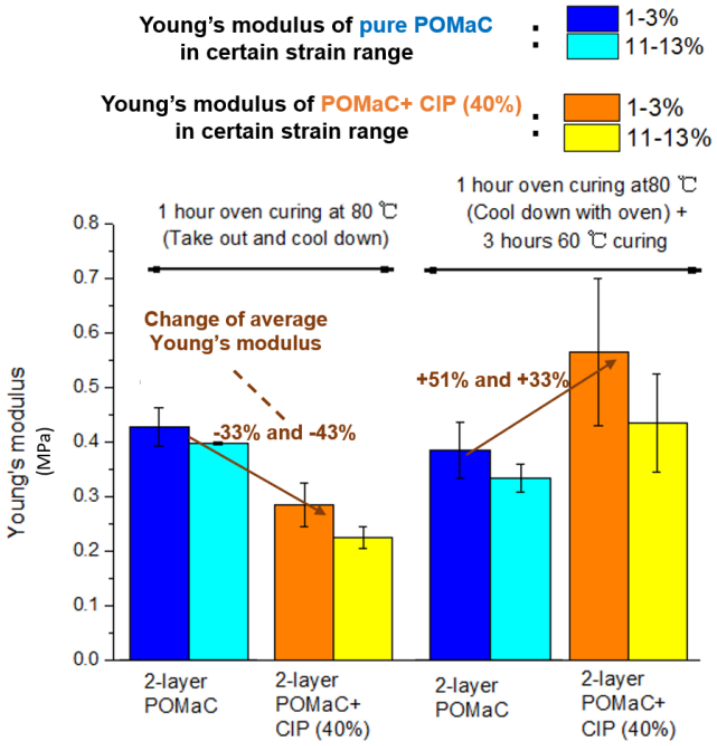

Figure 39. Mechanical property (Young's modulus) difference between pure POMaC samples and POMaC/CIP samples. 2-layer bonded samples which are bonded with heating conditions are compared.

POMaC is synthesized according to the detailed operations in protocol. Pre-POMaC batch 1 is cooled in atmosphere while batch 2 is cooled down with the heater which means that batch 1 experienced longer heating process than batch 2. Both of them are cooled until 100 ℃. As shown in figure 40, both 1-layer and 2-layer POMaC sample fabricated by batch 2 pre-POMaC show higher Young's modules than POMaC from batch 2 which means that longer heating process may induce higher polymerization of pre-POMaC and increase the stiffness of material.

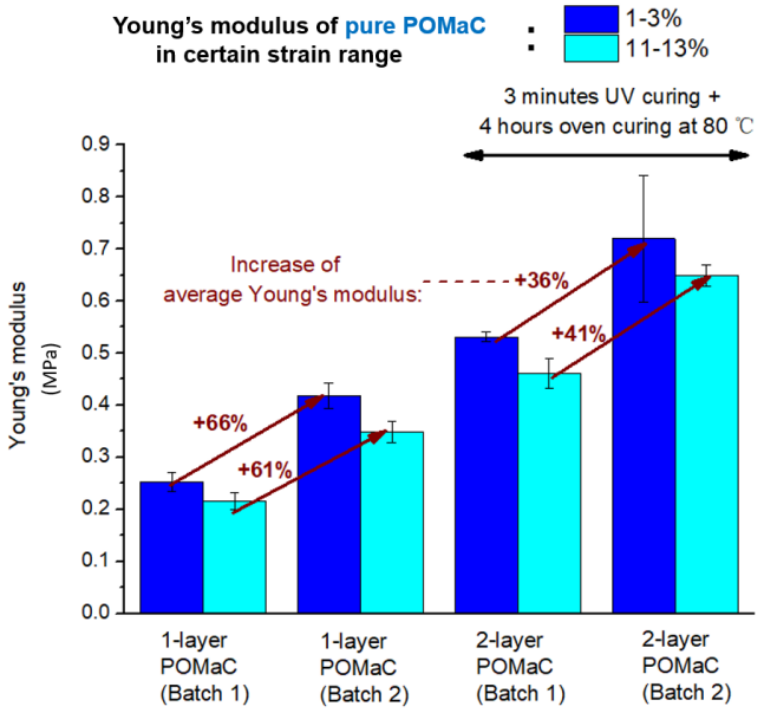

Figure 40. Mechanical property (Young's modulus) difference between samples which are fabricated by different batches (batch 1 and batch 2) of POMaC. After heating process, Batch 1 is cooled down in atmosphere while batch 2 is cooled down with the heater which means that POMaC batch 2 experienced longer heating treatment.

Table 4. Young's modulus values for all the samples in section 4.2.3.

	1-layer POMaC	2-layer bonded POMaC	1-layer POMaC (6.13 fabricated)	1-layer POMaC (6.24 fabricated)	1-layer POMaC/CIP (40%)	2-layer bonded POMaC	2-layer bonded POMaC/CIP (40%)	2-layer bonded POMaC	2-layer bonded POMaC/CIP (40%)	2-layer bonded POMaC
Batch number	Batch 1	Batch 1	Batch 2		Batch 2	Batch 2	Batch 2	Batch 2	Batch 2	Batch 2
Bonding condition for 2-layer sample		1 hour oven curing at 80 ℃ (Take out and cool down) + 3 minutes UV exposure				1 hour oven curing at 80 ℃ (Take out and cool down)		1 hour oven curing at 80 ℃ (cool down with oven) + 3 hours oven curing at 60 ℃		1 hour oven curing at 80 ℃ (Take out and cool down) + 3 minutes UV exposure
Young's modulus (MPa) of 1-	0.25	0.42	0.42	0.42	0.33	0.43	0.29	0.37	0.57	0.72
Standard deviation (MPa)	0.02	0.03	0.03	0.01	0.06	0.04	0.04	0.05	0.13	0.12
Young's modulus (MPa) of 11-13%	0.22	0.35	0.35	0.34	0.23	0.40	0.23	0.33	0.44	0.65
Standard deviation (MPa)	0.02	0.02	0.02	0.04	0.03	0.00	0.02	0.03	0.09	0.02

4.2.4 Degradation test

Bonded 2-layer pure POMaC samples and 2-layer POMaC/CIP samples are fabricated

based on the procedure in section 3.2. For 1-layer fabrication, 6 minutes exposure is applied to each side. After that, 2-layer POMaC is fabricated through bonding 2 POMaC samples together and 1 hour 80 ℃ baking + 3 hours 60 ℃ baking is applied to increase the adhesion between 2 layers. Totally, there are 9 2-layer pure POMaC samples and 9 2-layer POMaC/CIP samples. For pure POMaC and POMaC/CIP, 3 rounds of test will be carried out. Firstly, the properties of pure POMaC and POMaC/CIP samples are measured before being immersed in PBS which is referred as 'Week 0'. The properties are regularly measured after 7 days and 14 days degradation in 37 ℃ PBS solution. The measured samples are referred as 'Week 1' and 'Week 2'.

After fabrication, the masses of all the samples are measured so that the mass change can be recorded after degradation. The measurements are done after drying in desiccator where all the water is evaporated. For week-0 samples, its properties are measured immediately after fabrication without incubation in PBS. Remaining samples are immersed in PBS and transferred into the incubator (37 ℃). For week-1 samples and week-2 samples, before measurement, they are taken out from the beaker, cleaned in Di-water and dried by vacuum desiccator. Mass and length are measured after vacuum drying. Then, mechanical property (stress-strain curve) is obtained through DMA operation as detailed in section 3.5.

Samples incubated for different times are shown in figure 41. For week-0 samples, pure POMaC and POMaC/CIP shows similar dimension and are both soft. For week-1 sample, obvious shrinking and expanding can be seen in pure POMaC and POMaC/CIP samples respectively. Besides, POMaC/CIP samples become so brittle that it can be broken easily while pure POMaC samples are still ductile. After 1 more week, POMaC/CIP samples are crispy and even curly. Pure POMaC still maintain its elastomer feature.

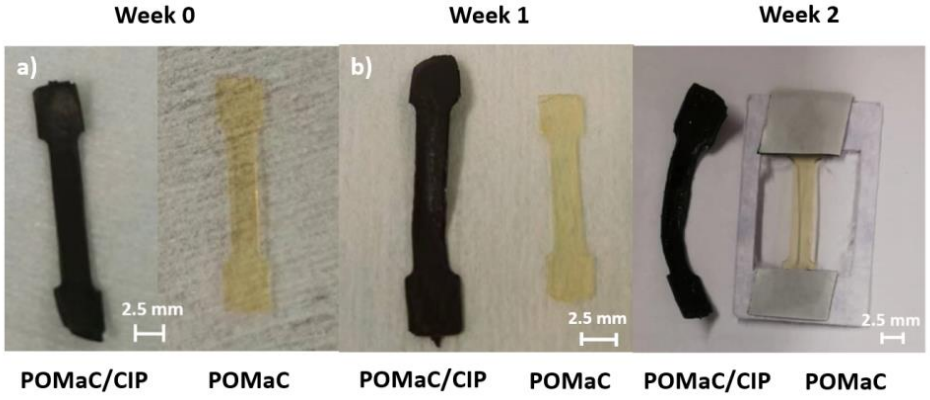

Figure 41. **Pictures of pure POMaC and POMaC/CIP which** a) did not experience PBS incubation b) are incubated in PBS solution for 1 week. c) are incubated in PBS solution for 2 weeks.

The mechanical property of all the samples is measured by DMA machine. Specific operation and parameter can be found in section 3.5. For week-1 samples, the stress-strain curves show obvious difference between POMaC/CIP and pure POMaC samples. All the measured curve are shown in figure 42. Incubated POMaC/CIP samples show higher Young's modulus and lower ultimate strain comparing with week-0 POMaC/CIP samples. Therefore, for POMaC/CIP samples incubated in PBS solution, it gradually loses its elastomer feature after certain incubation.

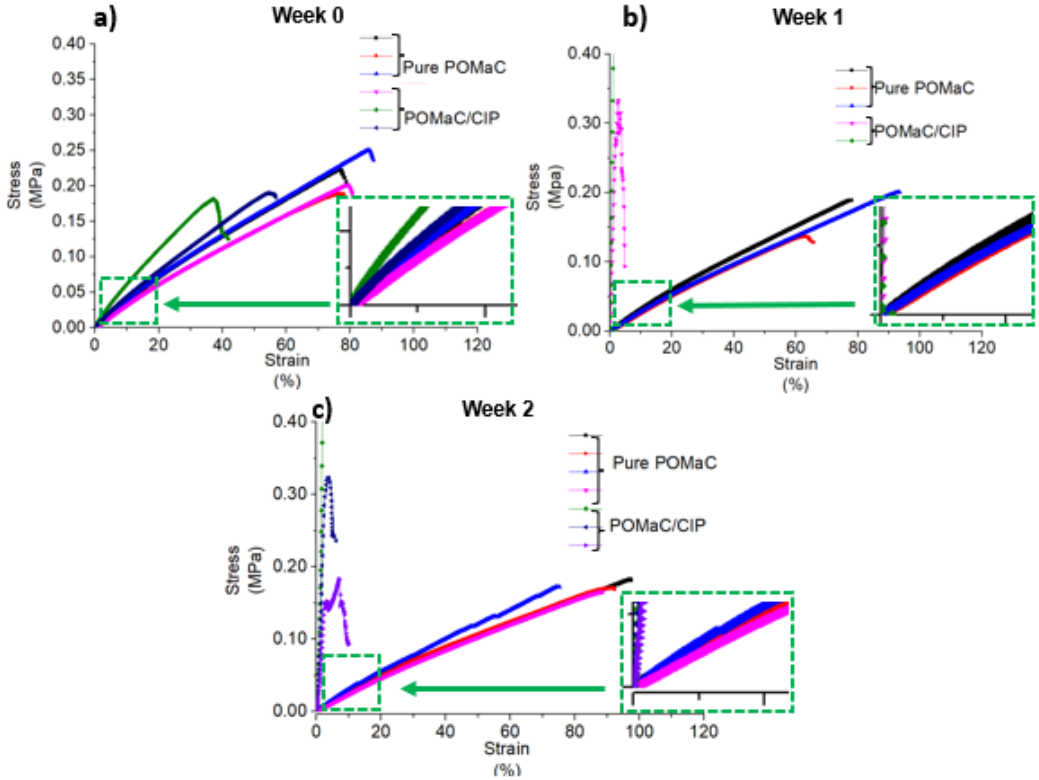

Figure 42. **Influence of degradation (incubating time) on mechanical property.** a) Stress-strain curves of bonded 2-layer pure POMaC samples and bonded 2-layer POMaC/CIP samples which did not experience 37 ℃ incubation in PBS solution. b) Stress-strain curves of bonded 2-layer pure POMaC samples and bonded 2-layer POMaC/CIP samples which experienced 37 ℃ incubation in PBS solution for 1 week. c) Stress-strain curves of bonded 2-layer pure POMaC samples and bonded 2-layer POMaC/CIP samples which experienced 37 ℃ incubation in PBS solution for 2 weeks.

Young's modulus values of pure POMaC and POMaC/CIP samples are calculated based on the stress-strain curves. Results are shown in figure 43 and table 4. POMaC/CIP samples break at a very small strain value (lower than 5%) so corresponding Young's modulus is calculated in the linear part of stress-strain curve. In figure 43, modulus value of POMaC /CIP samples show tremendous increasing after 1 week incubation while decrease is found in both 1-3% and 11-13% strain range of pure POMaC samples. For pure POMaC, it shows similar decreasing trend in Young's modulus as the POMaC results reported in [51]. Degradation of UV crosslinks caused by UV exposure and ester bond crosslinks caused by oven baking may be the main reason of decreasing Young's modulus. Especially, ester bonding may break due to hydrolysis during the immersion in PBS. For POMaC/CIP, increasing Young's modulus may result from the hindering effect of CIP which reduce the chemical bonding formation of pre-POMaC. Therefore, less bonding is formed in POMaC/CIP. It would be easier for POMaC/CIP to degrade in PBS. It was proved by Richard [31] that, if less chemical bonding is formed inside POMaC, the degradation speed would be faster. Therefore, the remaining CIP leads to much higher Young's modulus. It is because that CIP may work as the reinforcement phase which reinforce the composite material. Its reinforcing effect may get more obvious with degradation of POMaC matrix

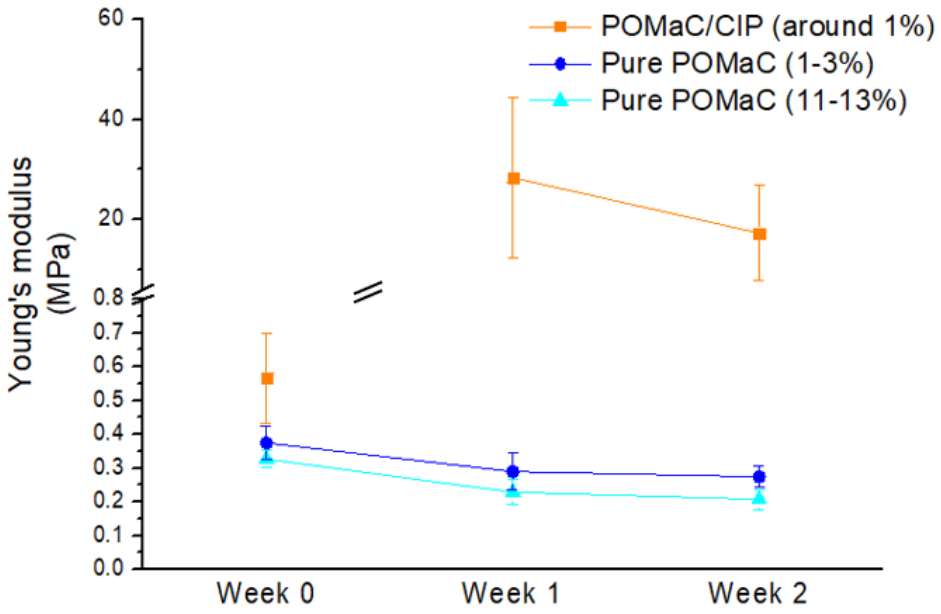

Figure 43. The Young's modulus values of pure POMaC samples and POMaC/CIP samples which are incubated in 37 ℃ PBS solution for different time. For incubated POMaC/CIP samples, it is so stiff that the ultimate strain value is lower than 11%. Therefore, the Young's modulus around 1% is calculated.

Table 4. Young modulus values of different samples which are incubated for different time.

	POMaC/CIP (around 1%)		**Pure POMaC (1-3%)**		**Pure POMaC (11-13%)**	
	Young's modulus value (MPa)	Standard deviation (MPa)	Young's modulus value (MPa)	Standard deviation (MPa)	Young's modulus value (MPa)	Standard deviation (MPa)
Week 0	0.57	0.13	0.37	0.05	0.33	0.03
Week 1	28	16	0.29	0.05	0.23	0.04
Week 2	17	9.5	0.27	0.03	0.21	0.03

Before incubation, the masses of all dried samples are recorded so that the mass change of each sample can be followed after incubation. The average mass of week-0 POMaC and POMaC/CIP samples is 39.8 mg and 23.8 mg respectively. It can be calculated that the mass of POMaC samples is 59.8% of POMaC/CIP sample which proved that almost all the remaining porogen, initiator and solvent should have been removed because 40% CIP is added into POMaC for POMaC/CIP sample. After 1-week and 2-week incubation, corresponding samples masses are measured again after vacuum desiccator drying. The total mass of different samples may fluctuate because of manual operation. Therefore,

except absolute mass change, relative change of mass is also calculated. Specific values of mass changes can be found in table 5.

In figure 44, POMaC/CIP samples show less mass decreasing than pure POMaC samples. As discussed before, there may be less crosslinks inside POMaC/CIP samples which make POMaC matrix degradation faster. However, the mass change of POMaC/CIP is smaller than pure POMaC. Maybe It is because that the degraded POMaC components remain in the POMaC/CIP sample because of CIP. The CIP works as 'pin' and restrain the leakage of degraded POMaC components. The second possibility is that the CIP structure inside POMaC matrix becomes more porous because of degradation. It attracts some solute in PBS solution and mitigate mass decrease of POMaC/CIP sample. The real reason needs to be proved by further investigation (eg, EDS and SEM).

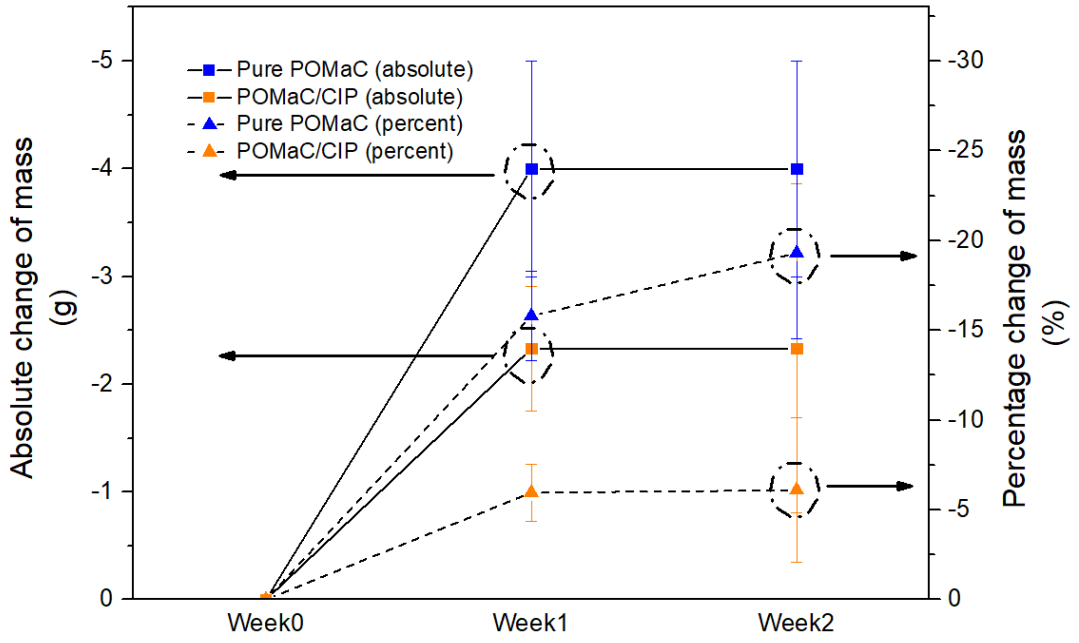

Figure 44. **Mass change of pure POMaC and POMaC/CIP which** a) did not experience PBS incubation b) are incubated in PBS solution for 1 week. c) are incubated in PBS solution for 2 weeks.

Table 5. The mass change of samples incubated for 1 week and 2 weeks.

	Pure POMaC		POMaC/CIP	
	mass △ value	Standard deviaton	mass △ value	Standard deviaton
Week 0 (absolute) (g)	0.00	0.00	0.00	0.00
Week 0 (percent) (%)	0.00	0.00	0.00	0.00
Week 1 (absolute) (g)	-4.00	1.00	-2.33	0.57
Week 1 (percent) (%)	-15.8	2.5	-5.96	1.58
Week 2 (absolute) (g)	-4.00	1.00	-2.33	1.52
Week 2 (percent) (%)	-19.3	4.78	-6.10	4.02

Length, width, and thickness values of week-0 pure POMaC samples are 10 mm, 2.5 mm and 0.6 mm respectively. Almost the same dimension is obtained in POMaC/CIP sample. After 1-week and 2-week incubation, dimension (length) changes of pure POMaC and POMaC/CIP samples are measured which is shown in figure 45. The change of width and thickness value is ignorable while length value is the main concerned parameter. Incubated POMaC/CIP samples show obvious increasing of length while pure POMaC samples shrunk a little bit which can also be found in figure 41. Length values of 1-week pure POMaC and POMaC/CIP are 9.3 mm and 12.8 mm. For 2-week samples, the values are 9.3 mm and 12.7 mm respectively which did not show obvious change comparing with the 1-week samples. Standard deviation is very small and is mainly resulted from the measurement operation of electronic ruler.

As discussed before, for pure POMaC hydrolysis is the main degradation method of it. During hydrolysis process, the broken ester bonding induces mass decrease and dimension shrinking because the broken parts flow out of the matrix material.

For POMaC/CIP, there are more voids in the network of CIP when degradation is ongoing. These porous network may attract PBS solute and absorb it. Therefore, absorbed particle or ion may enlarge POMaC/CIP sample and increase its mass comparing with pure POMaC. The real reason needs to be proved by further investigation (eg. EDS and SEM).

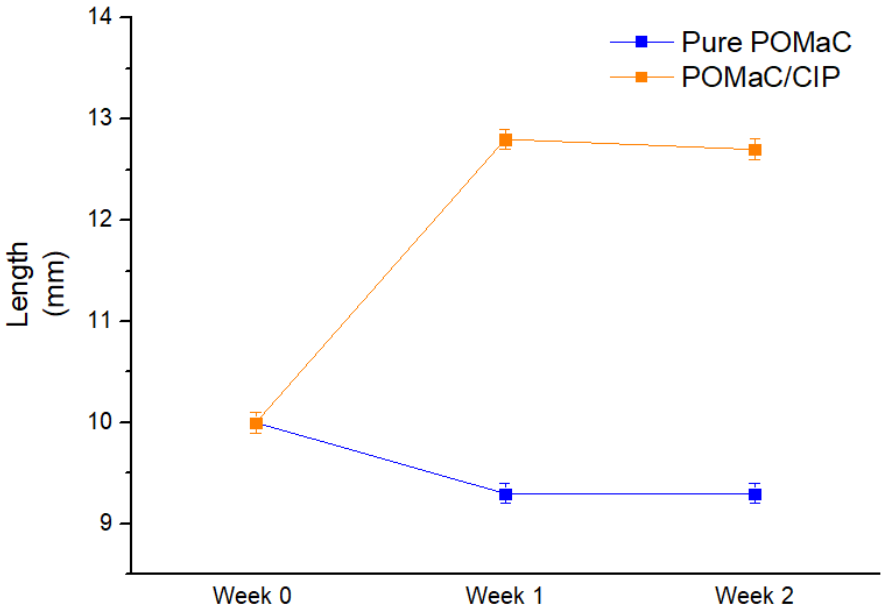

Figure 45. **Length value of pure POMaC and POMaC/CIP which** a) did not experience PBS incubation b) are incubated in PBS solution for 1 week. c) are incubated in PBS solution for 2 weeks.

4.3. POMaC/CIP film actuation

Both 1-layer POMaC/CIP and 2-layer POMaC/CIP samples are fabricated for actuation test. Perpendicular magnetic field is generated by dipole electromagnet. Sample is placed at the middle part of dipole electromagnet so that the sample is not influenced the non-uniform magnetic field at 2 ends. As explained in section 2, the deformations that are investigated in this thesis are bending of 1-layer POMaC/CIP sample and stretching of 2-layer POMaC/CIP sample. Besides, the deformation mechanisms are further explained through figure 28. In this section, the deformation of both 1-layer POMaC/CIP and 2-layer POMaC/CIP are investigated.

The actuation of 1-layer POMaC/CIP sample is shown in figure 46. It is bonded at the end of a glass rod. Sample shows no deformation in figure 46 a, when magnetic field is off. In figure 46 b, when field is applied 1-layer POMaC/CIP sample bends toward right side in order align CIP chain with the magnetic field [37]. In figure 46 c,d, samples is flipped and stuck to the glass bar again so CIP chain direction is the opposite of the sample shown in figure 46 a.b. When magnetic field is applied to the flipped sample it bends toward the opposite direction. It means that the deformation really depends on

the CIP chain distribution in POMaC/CIP.

In order to verify the assumption of stretching deformation in 2-layer POMaC/CIP sample, bonded sample is placed in the dipole electromagnet. When magnetic field is applied sample shows perpendicular stretching comparing with the sample that is not exposed to magnetic field. Although it does show perpendicular stretching the elongation is not obvious in figure 47 b. Higher magnetic field and low elasticity of sample may contribute to high strain.

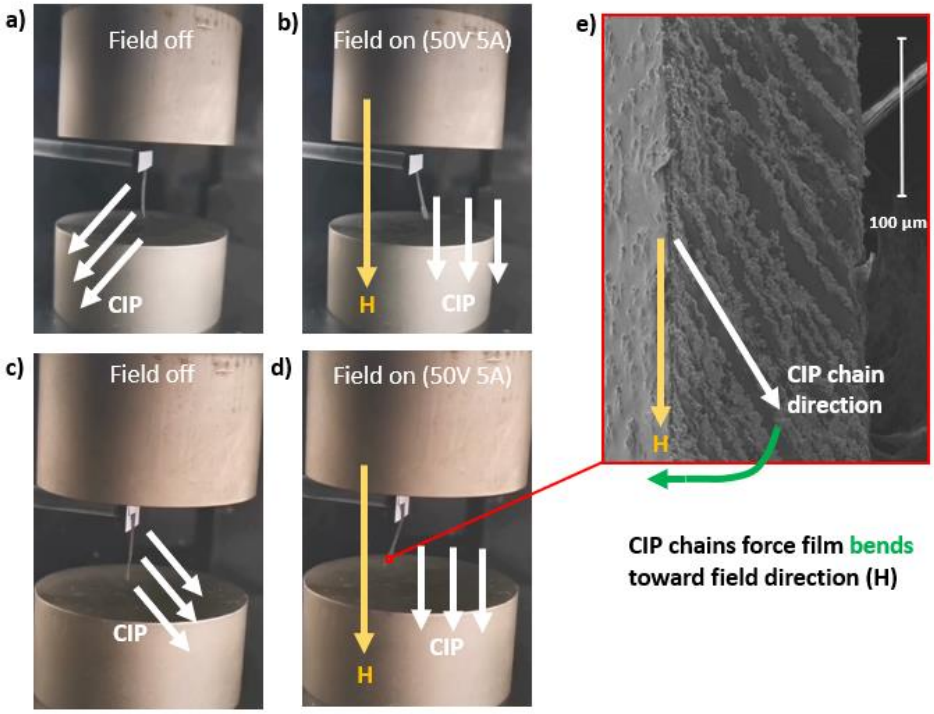

Figure 46. **Deformation of 1-layer POMaC/CIP hang between 2 electromagnets** where a) magnetic field is off. b) magnetic field is on. Deformation of flipped sample from figure a where c) magnetic field is off. d) magnetic field is on. e) SEM of 1-layer POMaC/CIP sample where the applied magnetic field, CIP chain direction and deformation direction are marked.

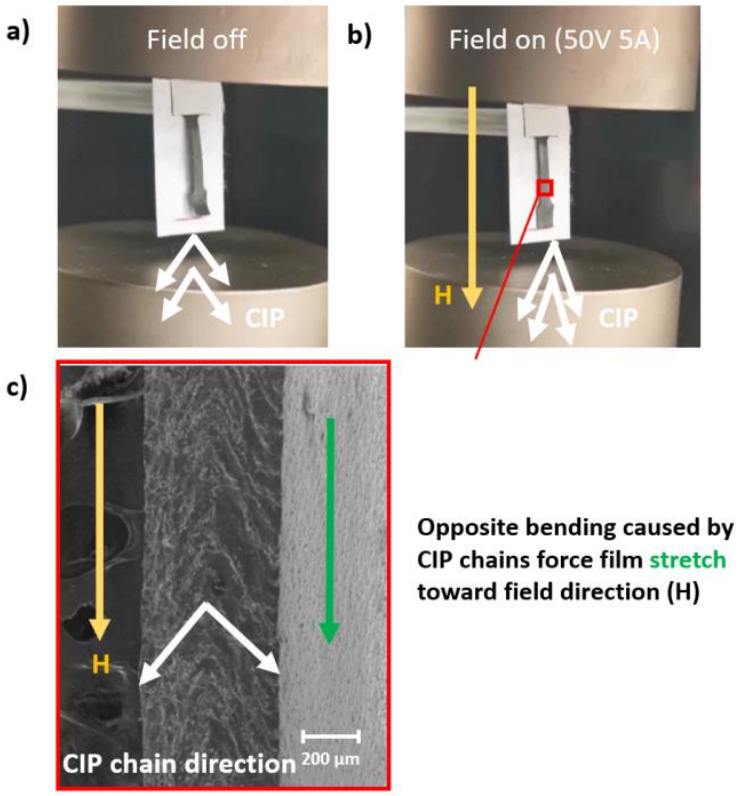

Figure 47. **Deformation of 2-layer POMaC/CIP hang between 2 electromagnets** where a) magnetic field is off. b) magnetic field is on. c) SEM of bonded 2-layer POMaC/CIP sample where the applied magnetic field, CIP chain direction and deformation direction are marked.

4.4 General discussion

In the thesis, POMaC/CIP scaffold is fabricated and characterized. The final application is to realized stretching actuation of POMaC/CIP substrate in OoC. In order to check the possibility of real application, magnetic property, mechanical property, degradation behavior and actuation situation are characterized.

As the driving for of magnetic deformation, the magnetic property of POMaC/CIP sample is important. Enough saturation magnetization is the one of the basic conditions for realizing stretching deformation of POMaC/CIP composite. The measured value is more than 70 Am^2/kg at both 300 K and 310 K. It is enough to realized bending, twisting and some other deformations as mentioned in some papers. In terms of mechanical property, the Young's modulus of 2-layer pure POMaC and POMaC/CIP does show significant difference if the bonding condition is suitable (eg. 1 hour 80 ℃ baking). It is crucial to have the Young's modulus of scaffold match the value of cultured tissue.

Otherwise, the mismatch may lead to inflammation and scar formation. The Young's modulus of 2-layer POMaC/CIP (1 hour 80 ℃ baking) is around 0.4 MPa which is similar to the value of many tissues. The value can also be further tuned by fabrication parameters. Therefore, fabricated POMaC/CIP fulfilled the mechanical requirement of OoC scaffold. The third consideration is degradation behavior of POMaC/CIP scaffold. As the tissue culturing process may take a few days, the degradation behavior of POMaC/CIP during this time is crucial. After 1-week immersion in PBS solution, POMaC/CIP does not show elastic performance any more. It means that the POMaC/CIP fabricated in the thesis cannot be used as scaffold to culture tissue for more than 7 days. The reason why this big change of mechanical property happens and how to improve it will be an important research direction in the future.

Finally, actuation test in magnetic field is carried out to test the propositions. 1-layer and 2-layer POMaC/CIP samples show bending and stretching deformation respectively. However, stretching is not obvious. Higher magnetic field, higher magnetization and more ductile scaffold can be the future research directions for improving the stretching deformation.

5

Conclusion and recommendation

The goal of this thesis is to fabricate a composite substrate which can generate stretching deformation when magnetic field is applied and characterize its mechanical, magnetic and degradation properties.

Pre-POMaC is synthesized successfully and mixed with CIP to fabricate POMaC/CIP thin film. The properties of thin films are characterized. For mechanical property, the Young's modulus of pure POMaC and POMaC/CIP (around 0.4 MPa) are both close to the Young's modulus of natural tissue. It means that POMaC/CIP substrate should be elastic enough to culture cells and generate stretching. The M-H curves of POMaC/CIP and CIP both show that strong response of CIP to magnetic field which is the foundation of magnetic actuation. The degradation results present that POMaC/CIP samples become much less elastic (lower Young's modulus and ultimate strain) after immersing in PBS which is the opposite to pure POMaC sample. Both 1-layer POMaC/CIP and 2-layer POMaC response to the perpendicular magnetic field where bending and small stretching is observed respectively.

In the future research, the following questions can be investigated to improve and supplement the research results in the thesis. Besides, these following researches can also accelerate the real application of POMaC/CIP substrate in OoC controlled by magnetic field.

Improve the stretching strain of 2-layer POMaC/CIP.

The stretching of 2-layer POMaC/CIP needs to be improved which is much lower than 15% now. Some aspects can be improved. The first one is to fabricate the more elastic substrate through adjusting the exposure parameter and CIP concentration. The second one is to have more magnetic torque. It may be realized by increasing the CIP

concentration and magnetic field intensity. Besides, the CIP chain generated by magnet is not very well aligned at some place which is far from magnet. Maybe electromagnet can be used to realized CIP chain distribution instead of magnet. Additionally, new substrate structure is also a possibility to get higher strain.

Investigate how CIP influence degradation

As shown in degradation section, POMaC/CIP gets much less elastic after 1-week immersing in PBS. Shorter immersing can be applied to the sample (eg. 1 day) and test its property change. Sample with different CIP concentration can also be fabricated and incubated in PBS. How does its degradation behavior change with CIP concentration?

Investigate how CIP influence mechanical property

As shown in mechanical test section, POMaC/CIP sample shows small decrease in Young's modulus comparing with POMaC sample which is deduced to be caused by the shadowing effect of CIP. This guess can be verified by changing CIP concentration and measuring the mechanical property change.

Bibliography

[1] B. Zhang and M. Radisic, “Organ-on-A-chip devices advance to market,” *Lab Chip*, vol. 17, no. 14, pp. 2395–2420, 2017, doi: 10.1039/c6lc01554a.

[2] D. Huh, B. D. Matthews, A. Mammoto, M. Montoya-Zavala, H. Yuan Hsin, and D. E. Ingber, “Reconstituting organ-level lung functions on a chip,” *Science (80-.).*, vol. 328, no. 5986, pp. 1662–1668, 2010, doi: 10.1126/science.1188302.

[3] F. J. O’Brien, “Biomaterials & scaffolds for tissue engineering,” *Mater. Today*, vol. 14, no. 3, pp. 88–95, 2011, doi: 10.1016/S1369-7021(11)70058-X.

[4] B. Zhang *et al.*, “Biodegradable scaffold with built-in vasculature for organ-on-a-chip engineering and direct surgical anastomosis,” *Nat. Mater.*, vol. 15, no. 6, pp. 669–678, 2016, doi: 10.1038/nmat4570.

[5] M. Shachar, N. Benishti, and S. Cohen, “Effects of mechanical stimulation induced by compression and medium perfusion on cardiac tissue engineering,” *Biotechnol. Prog.*, vol. 28, no. 6, pp. 1551–1559, 2012, doi: 10.1002/btpr.1633.

[6] Z. Qi, M. Zhou, Y. Li, Z. Xia, W. Huo, and X. Huang, “Reconfigurable Flexible Electronics Driven by Origami Magnetic Membranes,” *Adv. Mater. Technol.*, vol. 6, no. 4, pp. 1–10, 2021, doi: 10.1002/admt.202001124.

[7] H. S. Yu, J. J. Kim, H. W. Kim, M. P. Lewis, and I. Wall, “Impact of mechanical stretch on the cell behaviors of bone and surrounding tissues,” *J. Tissue Eng.*, vol. 7, 2016, doi: 10.1177/2041731415618342.

[8] M. S. F. Clarke and D. L. Feerack, “Mechanical load induces sarcoplasmic wounding and FGF release in differentiated human skeletal muscle cultures,” *FASEB J.*, vol. 10, no. 4, pp. 502–509, 1996, doi: 10.1096/fasebj.10.4.8647349.

[9] J. Liu, J. Liu, J. Mao, X. Yuan, Z. Lin, and Y. Li, “Caspase-3-mediated cyclic stretch-induced myoblast apoptosis via a Fas/FasL-independent signaling pathway during myogenesis,” *J. Cell. Biochem.*, vol. 107, no. 4, pp. 834–844, 2009, doi: 10.1002/jcb.22182.

[10] K. Kurokawa, S. Abe, K. Sakiyama, T. Takeda, Y. Ide, and K. Ishigami, “Effects of stretching stimulation with different rates on the expression of MyHC mRNA in mouse cultured myoblasts,” *Biomed. Res.*, vol. 28, no. 1, pp. 25–31, 2007, doi: 10.2220/biomedres.28.25.

[11] A. KUMAR, R. MURPHY, P. ROBINSON, L. WEI, and A. M. BORIE, “ Cyclic mechanical strain inhibits skeletal myogenesis through activation of focal adhesion kinase, Rac-1 GTPase, and NF-kB transcription factor ,” *FASEB J.*, vol. 18, no. 13, pp. 1524–1535, 2004, doi: 10.1096/fj.04-2414com.

[12] O. Iwanuma *et al.*, “Effects of mechanical stretching on caspase and IGF-1 expression during the proliferation process of myoblasts,” *Zoolog. Sci.*, vol. 25, no. 3, pp. 242–247, 2008, doi: 10.2108/zsj.25.242.

[13] A. Salameh *et al.*, “Right or left ventricular pacing in young minipigs with chronic atrioventricular block: Long-term in vivo cardiac performance, morphology, electrophysiology, and cellular biology,” *Circulation*, vol. 125, no. 21, pp. 2578–2587, 2012, doi: 10.1161/CIRCULATIONAHA.111.079087.

[14] T. Boudou *et al.*, “A microfabricated platform to measure and manipulate the mechanics of engineered cardiac microtissues,” *Tissue Eng. - Part A*, vol. 18, no. 9–10, pp. 910–919, 2012,

doi: 10.1089/ten.tea.2011.0341.

[15] D. Rappaport, D. Adam, P. Lysyansky, and S. Riesner, “Assessment of myocardial regional strain and strain rate by tissue tracking in B-mode echocardiograms,” *Ultrasound Med. Biol.*, vol. 32, no. 8, pp. 1181–1192, 2006, doi: 10.1016/j.ultrasmedbio.2006.05.005.

[16] G. Zhao, X. Bao, G. Huang, F. Xu, and X. Zhang, “Differential Effects of Directional Cyclic Stretching on the Functionalities of Engineered Cardiac Tissues,” *ACS Appl. Bio Mater.*, vol. 2, no. 8, pp. 3508–3519, 2019, doi: 10.1021/acsabm.9b00414.

[17] C. C. Chen, T. Y. Wong, T. Y. Chin, W. H. Lee, C. Y. Kuo, and Y. C. Hsu, “Systems biology approach to exploring the effect of cyclic stretching on cardiac cell physiology,” *Aging (Albany. NY).*, vol. 12, no. 16, pp. 16035–16045, 2020, doi: 10.18632/aging.103465.

[18] A. Marsano *et al.*, “Beating heart on a chip: A novel microfluidic platform to generate functional 3D cardiac microtissues,” *Lab Chip*, vol. 16, no. 3, pp. 599–610, 2016, doi: 10.1039/c5lc01356a.

[19] J. Zhang *et al.*, “Flexible anisotropic magneto-sensitive elastomer films with out-of-plane particle chain for bionic actuator,” *Compos. Part A Appl. Sci. Manuf.*, vol. 150, no. July, 2021, doi: 10.1016/j.compositesa.2021.106591.

[20] S. Qi, H. Guo, J. Fu, Y. Xie, M. Zhu, and M. Yu, “3D printed shape-programmable magneto-active soft matter for biomimetic applications,” *Compos. Sci. Technol.*, vol. 188, no. December 2019, 2020, doi: 10.1016/j.compscitech.2019.107973.

[21] J. Kim, S. E. Chung, S. E. Choi, H. Lee, J. Kim, and S. Kwon, “Programming magnetic anisotropy in polymeric microactuators,” *Nat. Mater.*, vol. 10, no. 10, pp. 747–752, 2011, doi: 10.1038/nmat3090.

[22] S. R. Goudu, I. C. Yasa, X. Hu, H. Ceylan, W. Hu, and M. Sitti, “Biodegradable Untethered Magnetic Hydrogel Milli-Grippers,” vol. 2004975, 2020, doi: 10.1002/adfm.202004975.

[23] W. Hu, G. Z. Lum, M. Mastrangeli, and M. Sitti, “Small-scale soft-bodied robot with multimodal locomotion,” *Nature*, vol. 554, no. 7690, pp. 81–85, 2018, doi: 10.1038/nature25443.

[24] M. Suter, “Photopatternable superparamagnetic nanocomposite for the fabrication of microstructures,” 2012.

[25] L. Hines, K. Petersen, G. Z. Lum, and M. Sitti, “Soft Actuators for Small-Scale Robotics,” *Adv. Mater.*, vol. 29, no. 13, 2017, doi: 10.1002/adma.201603483.

[26] A. Tokarev, J. Yatvin, O. Trotsenko, J. Locklin, and S. Minko, “Nanostructured Soft Matter with Magnetic Nanoparticles,” *Adv. Funct. Mater.*, vol. 26, no. 22, pp. 3761–3782, 2016, doi: 10.1002/adfm.201504443.

[27] A. A. Milne and W. Pooh, “Nanoparticles and thin films,” no. May, pp. 145–155, 2018.

[28] X. Cao, S. Xuan, S. Sun, Z. Xu, J. Li, and X. Gong, “3D Printing Magnetic Actuators for Biomimetic Applications,” *ACS Appl. Mater. Interfaces*, vol. 13, no. 25, pp. 30127–30136, 2021, doi: 10.1021/acsami.1c08252.

[29] J. Ge, Y. Hu, M. Biasini, W. P. Beyermann, and Y. Yin, “Superparamagnetic Magnetite Colloidal Nanocrystal Clusters **,” pp. 4342–4345, 2007, doi: 10.1002/anie.200700197.

[30] R. Li, L. Wang, D. Kong, and L. Yin, “Recent progress on biodegradable materials and transient electronics,” *Bioact. Mater.*, vol. 3, no. 3, pp. 322–333, 2018, doi: 10.1016/j.bioactmat.2017.12.001.

[31] R. T. Tran, P. Thevenot, D. Gyawali, J. Chiao, and J. Yang, “Synthesis and characterization of

a biodegradable elastomer featuring a dual crosslinking mechanism," pp. 2449–2461, 2010, doi: 10.1039/c001605e.

[32] Y. Kim, H. Yuk, R. Zhao, S. A. Chester, and X. Zhao, "Letter," 2018.

[33] M. Li, A. Pal, A. Aghakhani, A. Pena-Francesch, and M. Sitti, "Soft actuators for real-world applications," *Nat. Rev. Mater.*, vol. 0123456789, 2021, doi: 10.1038/s41578-021-00389-7.

[34] J. B. Tracy and T. M. Crawford, "Magnetic field-directed self-assembly of magnetic nanoparticles," *MRS Bull.*, vol. 38, no. 11, pp. 915–920, 2013, doi: 10.1557/mrs.2013.233.

[35] C. Peters, "Biodegradable Superparamagnetic Polymer Composites : From Material Identification to Device Application," no. 22886, 2015.

[36] M. Wang, L. He, and Y. Yin, "Magnetic field guided colloidal assembly," *Mater. Today*, vol. 16, no. 4, pp. 110–116, 2013, doi: 10.1016/j.mattod.2013.04.008.

[37] S. R. Mishra, M. D. Dickey, O. D. Velev, and J. B. Tracy, "Selective and directional actuation of elastomer films using chained magnetic nanoparticles," *Nanoscale*, vol. 8, no. 3, pp. 1309–1313, 2016, doi: 10.1039/c5nr07410j.

[38] S. Zhang, Y. Wang, R. Lavrijsen, P. R. Onck, and J. M. J. den Toonder, "Versatile microfluidic flow generated by moulded magnetic artificial cilia," *Sensors Actuators, B Chem.*, vol. 263, pp. 614–624, 2018, doi: 10.1016/j.snb.2018.01.189.

[39] H. Song *et al.*, "Reprogrammable ferromagnetic domains for reconfigurable soft magnetic actuators," *MicroTAS 2020 - 24th Int. Conf. Miniaturized Syst. Chem. Life Sci.*, pp. 1312–1313, 2020.

[40] T. Xu, J. Zhang, M. Salehizadeh, O. Onaizah, and E. Diller, "Millimeter-scale flexible robots with programmable three-dimensional magnetization and motions," *Sci. Robot.*, vol. 4, no. 29, 2019, doi: 10.1126/scirobotics.aav4494.

[41] H. Deng, K. Sattari, Y. Xie, P. Liao, Z. Yan, and J. Lin, "Laser reprogramming magnetic anisotropy in soft composites for reconfigurable 3D shaping," *Nat. Commun.*, vol. 11, no. 1, pp. 1–10, 2020, doi: 10.1038/s41467-020-20229-6.

[42] D. C. Stanier, J. Ciambella, and S. S. Rahatekar, "Fabrication and characterisation of short fibre reinforced elastomer composites for bending and twisting magnetic actuation," *Compos. Part A Appl. Sci. Manuf.*, vol. 91, pp. 168–176, 2016, doi: 10.1016/j.compositesa.2016.10.001.

[43] F. Tsumori, A. Saijou, T. Osada, and H. Miura, "Development of actuation system for artificial cilia with magnetic elastomer," *Jpn. J. Appl. Phys.*, vol. 54, no. 6, 2015, doi: 10.7567/JJAP.54.06FP12.

[44] J. Feng, S. Xuan, L. Ding, and X. Gong, "Magnetoactive elastomer/PVDF composite film based magnetically controllable actuator with real-time deformation feedback property," *Compos. Part A Appl. Sci. Manuf.*, vol. 103, pp. 25–34, 2017, doi: 10.1016/j.compositesa.2017.09.004.

[45] L. Wang, D. Zheng, P. Harker, A. B. Patel, C. Fei, and X. Zhao, "Evolutionary design of magnetic soft continuum robots," vol. 118, no. 21, pp. 1–8, 2021, doi: 10.1073/pnas.2021922118.

[46] B. Zhang, B. F. L. Lai, R. Xie, L. D. Huyer, M. Montgomery, and M. Radisic, "Microfabrication of angiochip, a biodegradable polymer scaffold with microfluidic vasculature," *Nat. Protoc.*, vol. 13, no. 8, 2018, doi: 10.1038/s41596-018-0015-8.

[47] Luutzen, "Master Thesis Luutzen stress-stress measurements.pdf." .

[48] ufacturi C. B. Manng, C. R. Specimens, and T. Determina-, "Standard Test Methods for

Vulcanized Rubber and Thermoplastic Elastomers —,” pp. 1–14, 2009.

[49] M. M. Schmauch, S. R. Mishra, B. A. Evans, O. D. Velev, and J. B. Tracy, “Chained Iron Microparticles for Directionally Controlled Actuation of Soft Robots,” *ACS Appl. Mater. Interfaces*, vol. 9, no. 13, pp. 11895–11901, 2017, doi: 10.1021/acsami.7b01209.

[50] R. M. Erb, R. Libanori, N. Rothfuchs, and A. R. Studart, “Three Dimensions by Using Low Magnetic Fields,” *Science (80-.).*, vol. 335, no. January, pp. 199–204, 2012.

[51] C. M. Boutry *et al.*, “A stretchable and biodegradable strain and pressure sensor for orthopaedic application,” *Nat. Electron.*, vol. 1, no. 5, pp. 314–321, 2018, doi: 10.1038/s41928-018-0071-7.

A

Protocol

Fabrication of PDMS molds

1- Design the mold in SolidWork/SolidEdge and 3D print the mold in Asiga 3D printer. 3D-printed molds are stuck on single wafer box.

CRITICAL STEP: Make sure the molds are flat on the wafer box. Otherwise, liquid PDMS may flow into uneven part and make your PDMS mold out of flatness.

2- Put the wafer box full of 3D-printed molds and a little dish filled with 5-10 droplets silane in the vacuum desiccator. It would be better if this salinization process can last overnight. Vacuum is applied for at least 4 hours.

3- Weigh 10-30 g PDMS silicone elastomer with curing agent at a mass ratio of 20:1 in disposable plastic cup. Close the cup and put the mixture in the Speed Mixer.

4- Put PDMS/curing agent mixture in vacuum desiccator for at least 30 minutes to remove the bubbles caused by mixing process.

5- Pour PDMS/curing agent mixture onto the silanized 3D-printed molds. Put the wafer box in vacuum desiccator for another 30 minutes to remove the bubbles caused by pouring process.

6- Put the wafer box into 80 ℃ oven for 1.5-hour curing.

Chemical synthesis of POMaC prepolymer

7- Clean 250-mL three-necked round-bottom flask by acetone/IPA/Di water in sequence. Fully dry it through N_2 flow. If possible, it would be better to dry it in oven for a few hours.

8- Weigh out the reactants—1,8 octanediol, citric acid and maleic anhydride—at a molar ratio of 5:1:4. Put these 3 chemicals into the flask together with a magnetic stir bar. For 250-mL flask, 30 g maleic anhydride, 14.7 g citric acid and 55.9 g 1,8

octanediol are recommended. For bigger flask, large amount of chemicals can be used to synthesize more Pre-POMaC.

CRITICAL STEP: Certain space should be left for 1,4-diaxone which will be poured into the flask as solvent.

9- Put flask onto the heater. Configurate the synthesis setup based on figure S1, i. Temperature detector and N_2 gun are fix at left and right side. The cooling water tube is fixed at the middle.

CRITICAL STEP: For the middle neck, a little bit petroleum jelly glue can be coated around the neck so that better sealing can be ensured. A needle is punctured in to the rubber lid of cooling water tube which works as an outlet of N_2 flow. Make sure that the inlet and outlet connected to cooling water tube is sealed well so that the water will not flow out.

10- Start N_2 purge. N_2 flow is applied for 3 minutes so that the air inside the flask can be expelled. Then, N_2 flush is replace by vacuum which suck the remaining air away. Vacuum is applied for another 3 minutes. Repeat above 2 operation 3 times.

CRITICAL STEP: During vacuum process, put your finger on the punctured needle so that a closed space is formed. Do not open the N_2 flush too much otherwise the rubber lid will be pushed away.

11- Turn on the heater. Make sure N_2 flow is always on during heating process. Gradually increase the target temperature from 40, 60, 90, 120 finally to 140 ℃. When chemicals start to melt, turn on the magnetic stir for more homogenous heating.

CRITICAL STEP: Make sure the temperature detector is contact with the bottom of flask. After magnetic stirring starts, move the temperature detector up and make sure that the temperature detector is immersed as much as possible. When chemical start to melt, you can used temperature detector to stir the chemical a little bit to avoid local heating.

12- When temperature is stable at 140 ℃, keep reacting for 3 hours.

13- Turn off the heater and take the flask out off the heater for cooling down.

14- Prepare 1,4 dioxane solvent for dissolving pre-POMaC. 1 ml 1,4 dioxane is needed

for dissolving every 1 g chemicals. For the chemical weight mentioned in step 8, 100.6 ml 1,4 dioxane is poured in the flask.

CRITICAL STEP: Pour 1,4 dioxane in the flask full of POMaC pre-polymer, when temperature is around 100 ℃ so that the solubility of polymer is still high.

15- Turn on the magnetic stirring, make sure pre-POMaC is fully dissolved. Keep stirring for 10 minutes.

16- Pour dissolved pre-POMaC in separatory funnel. Put the funnel above a beaker filled with 2 L Di-water (corresponding to the chemical amount in step 8). Specific configuration can be found in figure S2, i.

17- Open the switch. Around 2 droplets of pre-POMaC fall down every second.

CRITICAL STEP: During purification process, chemicals floating on the surface of beaker are removed periodically (every 30 seconds) so that they do not accumulate and fall.

18- After purification, pour the water out of beaker. Pre-POMaC stays at the bottom of the beaker. Transfer the precipitated pre-POMaC to a clean flask.

19- Overnight N_2 flow is applied to the pre-POMaC inside the flask so that the residual water and 1,4-dioxane can be removed.

CRITICAL STEP: Successfully synthesized pre-POMaC should be transparent and viscous. If it still looks white, longer N_2 flow can be applied.

20- Purified and dried pre-POMaC can be stored in the refrigerator (around 4 ℃). Wrap the container with aluminum foil to protect it from light.

Pure POMaC and CIP/POMaC sample fabrication

21- Peel off the PDMS layer from 3D-printed mold. Cut the PDMS mold one by one and clean its surface by Scotch tape.

22- Cap the feature layer of PDMS mold on glass slide.

CRITICAL STEP: 4 PDMS molds can fixed on 1 standard glass slide. For pure POMaC sample, normal exposure is done on this substrate. For CIP/POMaC sample fabrication, 1 standard glass slide is split into 2 pieces otherwise a glass slide is too big to be accommodated on the magnet.

23- Mix POMaC prepolymer with Poly(ethylene glycol) dimethyl ether (PEGDM porogen) at a 2:3 (POMaC/PEGDM porogen) weight

ratio. Then, add 5% (wt/vol) initiator into above mixture. For pure POMaC, that is all the chemicals needed. For CIP/POMaC, certain percentage CIP is added into the mixture. I used 40% in this protocol.

CRITICAL STEP: Usually, for 10 samples (25 mm, 3 mm, 0.3 mm) fabrication, 1.5 g pure POMaC plus corresponding chemicals would be enough.

24- Mix the reagent with a spatula for 6 minutes on the hotplate. Rotate the knob toward the '80' marker. The heating temperature ranges from 80-120 ℃ based on my measurement.

25- Pour the mixture into a 5 ml syringe. Inject the mixture into PDMS mold fabricated in step 22 through the inlet.

CRITICAL STEP: Make sure that the size of needle is suitable for the inlet size.

26- For pure POMaC samples, put injected molds under the UV light Philips HB 175 with 4 lights (philips cleo 15w) and turn on the lamp. For CIP/POMaC samples, put the samples (number = 2) on the magnet holder shown in figure S3. For both situations, 6 minutes UV exposure is applied to each side of sample (Totally 12 minutes). After 6 minutes exposure, flip the samples to make sure that the exposure is homogeneous.

CRITICAL STEP: 6 minutes is an experimental time for pure POMaC and CIP (40%) /POMaC. Elastic film can be cured according above exposure operation. It can be changed according to the material property that you need. For CIP/POMaC, in order to generate chain distribution, the way you flip sample is important. Flip the sample like what is doing in figure S3.

27- Uncap the PDMS mold from glass slide.

CRITICAL STEP: Do this step carefully. Thin film may remain on the glass slide or inside PDMS mold. For the latter, use tweezer to pick sample out of the mold.

28- For 1-layer sample fabrication, put it in PBS solution overnight to leach out the remaining initiator and porogen. For 2-layer bonded sample fabrication, first align 2 layers with each other and gently press them together. Put pressed 2-layer sample in the

oven at 80 ℃ for 1 hour to further bond 2 layers. Put the bonded 2-layer sample in PBS solution overnight.

29- Take sample out of PBS and wash it with DI-water.

30- Dry it with cleanroom paper. Then, put it the vacuum desiccator to further evaporate remaining water.

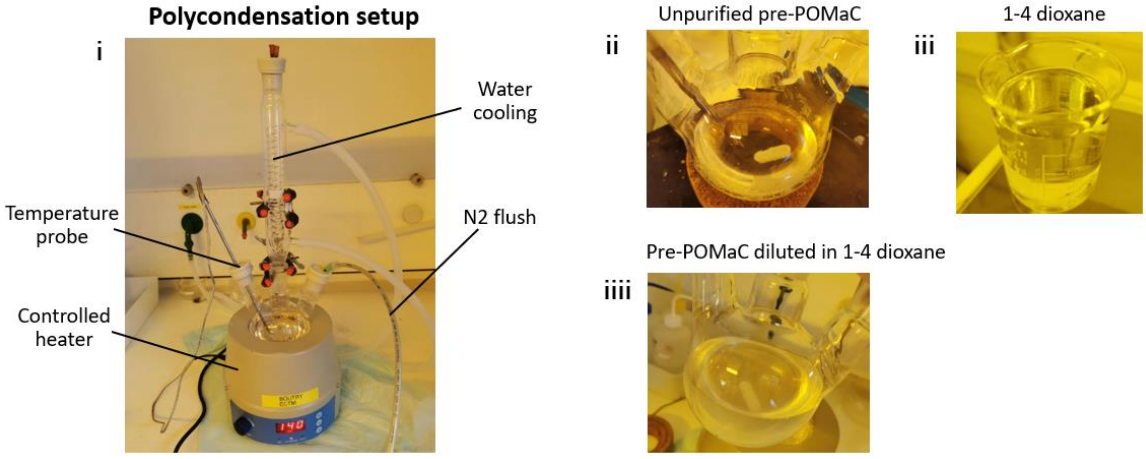

Figure S1. **Pre-POMaC heating synthesis.** (i) Polycondensation setup used for synthesizing POMaC. (ii) Unpurified pre-POMaC which is obtained through 3 hours heating under 140 ℃ in the setup in figure S1 (i). (iii) 1-4 dioxane is used as solvent for dissolving pre-POMaC. (iiii) pre-POMaC solution obtained by pouring 1-4 dioxane in unpurified pre-POMaC. 1-4 dioxane is poured in pre-POMaC when the temperature of POMaC is 100 ℃. Magnetic stirring is applied for 10 minutes for better dissolving.

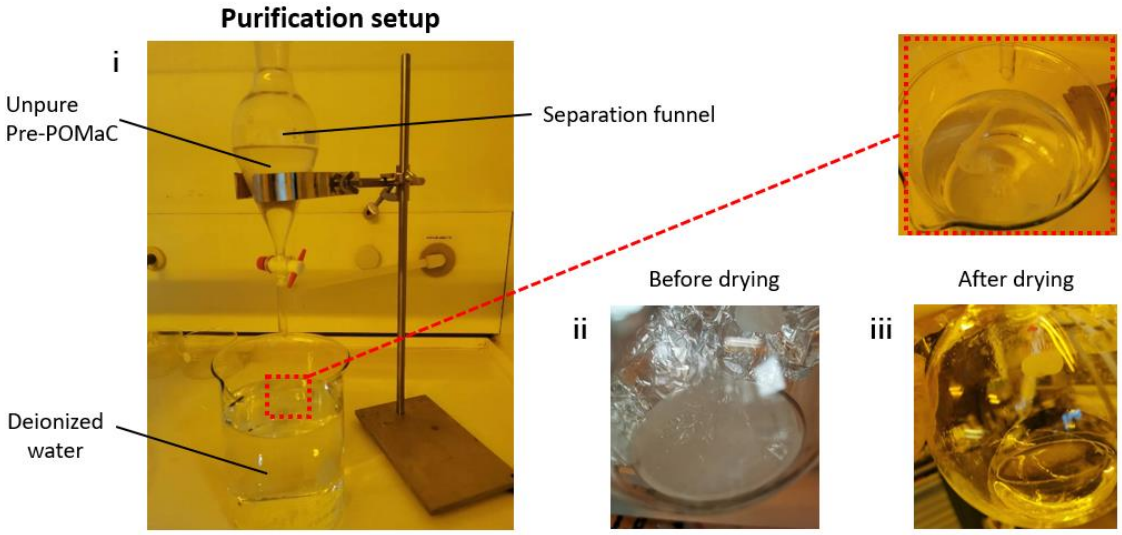

Figure S2. **Pre-POMaC purification and drying process.** (i) Purification setup used for separating pre-POMaC (at the bottom of beaker) from monomer and pre-POMaC which are not fully polymerized (on the top of beaker). 2L water is filled in the beaker. (ii) pre-POMaC obtained at the bottom of beaker is transferred to a new flask. (iii) N_2 gas flow is applied to pre-POMaC overnight

in order to get rid of 1,4-dioxane and water.

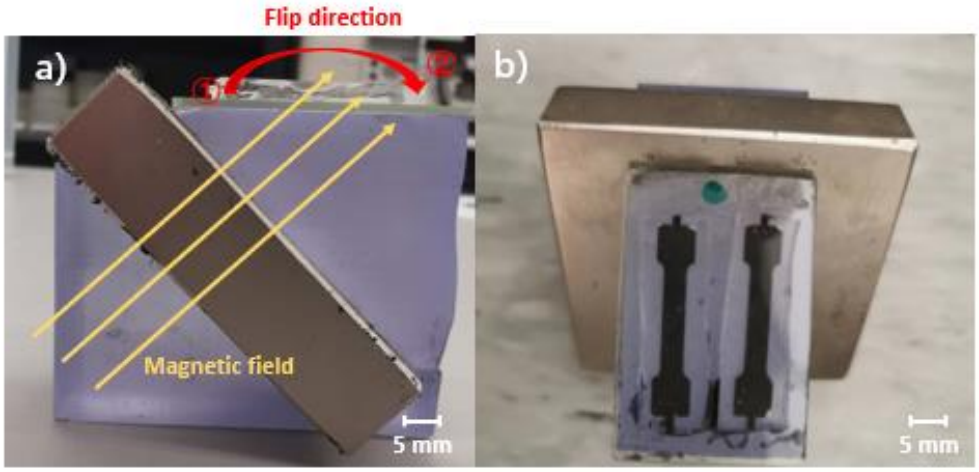

Figure S3. **Configuration used for magnetizing CIP/POMaC samples and genrrating CIP particle distribution.** a) Side view. b) Top view.